



BOTSWANA UNIVERSITY OF AGRICULTURE & NATURAL RESOURCES

A Geospatial assessment of soil erosion risk and soil fertility changes due to ISPAAD programme: **A case study of Dinogeng Agricultural Extension Area, Kgatleng District.**

A research thesis submitted to the Department of Agricultural & Bio-systems Engineering in partial fulfilment of the requirements of the award of the Masters of Science Degree in Agricultural Engineering (Land Use Planning) Stream.

By

Lucky Sitayelo

ID Number: 201500019

June 2022

Main Supervisor: Prof. B. Kayombo

Co - Supervisors:

Prof. C. Patrick

Ms E. Kgosiesele

**CERTIFICATION**

---

Main Supervisor's Name and Signature

---

Date

---

Co-Supervisor's Name and Signature

---

Date

---

Co-Supervisor's Name and Signature

---

Date

---

Head of Department's Name and Signature

---

Date

**APPROVAL**

---

Main Supervisor's Name and Signature

---

Date

---

Co-Supervisor's Name and Signature

---

Date

---

Co-Supervisor's Name and Signature

---

Date

---

Head of Department's Name and Signature

---

Date

---

Dean of Faculty's Name and Signature

---

Date

**STATEMENT OF ORIGINALITY**

The work contained in this thesis/dissertation was compiled by the author at the Botswana University of Agriculture & Natural Resources between January 2019 and June 2022. This thesis/dissertation has been submitted in partial fulfilment of the requirements for an MSc degree at Botswana University of Agriculture & Natural Resources (BUAN). It is original except where the references are made and it will not be submitted for the award of any other academic degree, diploma, or certificate of any other institution or University.

---

Author's Name and signature

---

Date

## **ACKNOWLEDGEMENTS**

I am grateful beyond words on how to thank my main supervisor Professor B. Kayombo for his continuous encouragement and professional guidance throughout all the stages of research and the writing of this thesis. Without his consistent and illuminating instruction in reviewing my work, this thesis could not have reached its present form. I would also like to express my deepest gratitude and appreciation to my co-supervisors Professor C. Parick and Ms E. Kgosiesele for their unreserved support in providing valuable and constructive comments to my thesis from the beginning to end. Appreciation also goes to Botswana University of Agriculture and Natural Resources (BUAN) more especially the Department of Agricultural and Bio-Systems Engineering (ABE) and BUAN Library for the coordination and provision of all resources required for the completion of this work. I certainly thank BUAN for the education and cultivation I received towards the completion of my Master program.

I would like to highly acknowledge the Principal Ms C. Male and staff of St Joseph's College for their support in pursuit of my part-time studies at BUAN. I could also not forget the Ministry of Agricultural Development and Food Security for providing digital soil data, Department of Agricultural Research Soil Analytical Laboratory, Agricultural extension officers and the Agricultural District Headquarters at Mochudi for providing soil test reports, the Department of Forestry and Range Resources (DFRR) of the Ministry of Environment, Wildlife and Tourism for providing forest information for Kgatleng District from their GIS database, the Department of Meteorological Services (DMS) for providing climatic data and the United States Geological Survey (USGS) Earth Resources Observation Systems (EROS) for providing satellite images of the study area. Botswana Secondary School Teachers Union (BOSETU) is also acknowledged for the financial support towards a portion of my thesis.

I greatly acknowledge Prof F. Meulenberg, Dr S. Moroka, Mr. G.Yuyi, Mr. I. Makoi, Mr. S.M. Moesi and fellow graduate student Issa Kaduyu for their technical and scientific help and support. My family and friends also helped me a lot throughout my graduate study. I wish to express my warmest gratitude to my wife Gontse and kids Nako and Unami, parents Sarah Sitayelo and Richard Sitayelo, maternal grandfather Mr. Brown Mphinyane for their endless love and support in my journey of life. I am also grateful to my Uncle Dr.Nchidzi W. Mphinyane and Cousin Miliko Laba for their care, encouragement and inspiration. I raise the value of all the backing and encouragement that lead to completion of this dissertation work. Last but not list, I would like to thank the Almighty GOD for making everything possible.

## **DEDICATION**

I dedicate my dissertation work to my family and those who supported me. A special feeling of gratitude goes to my loving wife, Gontse who encouraged me to pursue my dreams and finish my dissertation. I also dedicate this work and give special thanks to my cousin Miliko Laba, and my wonderful kids Umami and Nako for being there for me throughout the entire master's program. Both of you have been my best cheerleaders. This work is also devoted to Ratshipa Ramatlhakola and my sister Iris Sitayelo for the inspiration for me to pursue my master's degree, and Botswana Secondary School Teachers Union (BOSETU) for the financial support towards part of my thesis.

## **ABSTRACT**

This study was conducted in Dinogeng Agricultural Extension Area (DAEA) in the Kgatleng District located in the eastern part of Botswana. The main objective of this study was to assess soil erosion risk and soil fertility changes before and after inception of the Integrated Support Programme for Arable Agricultural Development (ISPAAD) programme using geospatial techniques. The study determined land use land cover changes (LULCC) using Geographical Information System (GIS) and Remote Sensing (RS), analysed soil fertility changes and mapped out soil erosion risk areas using Soil Loss Estimation Model for Southern Africa (SLEMSA) and GIS. Landsat 5 and 8 satellite images of 2006 and 2020 were obtained for the purpose of land cover classification. In a 14-year span (2006-2020), land use land cover (LULC) of DAEA changed markedly. Cultivated land and bare areas increased by 19.4 and 18.3 % whereas shrub land and forest areas decreased by 36.9 and 0.7 %, respectively. It is evident that the ISPAAD programme contributed to land degradation during the period. The chemical properties of the soils for eighteen farmers in Dinogeng were compared with data obtained from national soil map of Botswana (1988) scale 1: 250 000. The results showed an average decline of 1.55 for soil reaction (pH), 0.16 % for organic carbon (OC) and 6.75 Cmol/kg for cation exchange capacity (CEC). The rate of soil loss was determined by utilizing information on rainfall energy (E) using interpolation of rainfall data, topography using Digital Elevation Model (DEM), soil erodibility (F) using soil map and LULC data using satellite images within the SLEMSA framework. The results indicated that 88% of DAEA has low to moderate soil erosion risk ( $0 - 2 \text{ tha}^{-1}\text{yr}^{-1}$ ). Only 12% of the study area experience very high to extreme high erosion risk ( $5 - \geq 10 \text{ tha}^{-1}\text{yr}^{-1}$ ) along the streams, at steep slopes and areas of bare land. It is a common practice for conservation measures to be applied on areas with high soil loss. Furthermore, the findings from this study may be useful to guide the development of functional soil conservation and land use planning as well as soil fertility management plan for Dinogeng Agricultural Extension Area.

**Key words:** Dinogeng Agricultural Extension Area, Botswana, ISPAAD, Soil erosion, GIS, RS, SLEMSA, LULC, Soil fertility.

**LIST OF TABLES**

Table 4.1. LULC class description for the classification process.....	38
Table 4.2. The LULC change detection for 2006 and 2020 of Dinogeng .....	40
Table 4.3. Error matrix for 2006 classified map.....	43
Table 4.4. Error matrix for 2020 classified map.....	44
Table 4.5. Soil characteristics of the study area.....	47
Table 4.6. Soil parameters in the study area before and after ISPAAD .....	48
Table 4.7. Estimation of SOM content in the study area before and after ISPAAD .....	49
Table 4.8. Estimated soil erosion risk in Dinogeng for 2020 LULC.....	56

**LIST OF FIGURES**

Fig. 2.1. Framework for SLEMSA model .....	11
Fig.4. 1 LULC classification maps (2006 and 2020).....	39
Fig.4. 2 Location of farmer's fields and soils of Dinogeng.....	45
Fig.4. 3 Topographic Ratio input factors and DEM .....	46
Fig.4. 4 Topographic ratio (X factor) map.....	51
Fig.4. 5 Principal K and input factors .....	53
Fig.4. 6 Spatial distribution of (a) LULC for 2020 and (b) Crop ratio .....	54
Fig.4. 7 Spatial distribution of annual soil loss of Dinogeng.....	55
Fig.4. 8 Soil erosion risk map for Dinogeng.....	56

## LIST OF ACRONYMS AND ABBREVIATIONS

AGRA	Alliance for Green Revolution in Africa
ALDEP	Arable Land Development Programme
ARAP	Accelerated Rain-fed Arable Programme
C	Crop Ratio
CE	Commission error
CEC	Cation Exchange Capacity
CREAMS	Chemicals, Runoff, and Erosion from Agricultural Management Systems
DAEA	Dinogeng Agricultural Extension Area
DFRR	Department of Forestry and Range Resources
DEM	Digital Elevation Model
DMS	Department of Meteorological Services
E	Rainfall Energy
EUROSEM	European Soil Erosion Model
F	Soil Erodibility Factor
FAO	Food and Agriculture Organisation
GDP	Gross Domestic Product
GIS	Geographical Information System
GPS	Global Position System
IDW	Inverse Distance Weighting
ISPAAD	Integrated Support Programme for Arable Agricultural Development
<i>K</i>	Cohen's Kappa coefficient
K	Principal Factor
LULC	Land use land cover
LULCC	Land use land cover change
MAP	Mean Annual Precipitation
MLC	Maximum Likelihood Classification
OC	Organic carbon
OE	Omission error
OM	Organic Matter
OSU	Ohio State University Extension
PA	Producer's Accuracy

pH	Soil Reaction
RS	Remote Sensing
RUSLE	Revised Universal Soil Loss Equation
SLEMSA	Soil Loss Estimation Model for Southern Africa
SOC	Soil Organic Carbon
SOM	Soil Organic Matter
SRTM	Shuttle Radar Topography Mission
SSA	Sub-Saharan Africa
SWEAP	Soil Water Erosion Assessment Program
UA	User's Accuracy
USDA	United States Department of Agriculture
USGS	United States Geological Survey
USLE	Universal Soil Loss Equation
UTM	Universal Transverse Mercator
X	Topographic Factor
Z	Predicted Mean Annual Soil Loss

## TABLE OF CONTENTS

### Table of Contents

CERTIFICATION .....	ii
APPROVAL .....	iii
STATEMENT OF ORIGINALITY .....	iv
ACKNOWLEDGEMENTS .....	v
DEDICATION .....	vi
ABSTRACT .....	vii
LIST OF TABLES .....	viii
LIST OF FIGURES .....	ix
LIST OF ACRONYMS AND ABBREVIATIONS .....	x
TABLE OF CONTENTS .....	xii
CHAPTER 1: INTRODUCTION .....	1
1.1 Status of Food Security in Sub-Saharan Africa (SSA) .....	1
1.2 Status of Traditional Arable Agriculture in Botswana .....	2
1.3 Brief Description of ISPAAD Programme .....	4
1.4 Statement of the Problem .....	5
1.5 Significance of the Proposed Study .....	6
1.6 Purpose of the Proposed Study .....	6
1.7 Aim of the Study .....	7
1.7.1 Specific Objectives of the Study .....	7
CHAPTER 2: LITERATURE REVIEW .....	8
2.1 Land use changes .....	8
2.1.1 Land-Use/Land-Cover Change .....	8
2.2 Land degradation .....	9
2.2.1 Soil erosion process and contributing factors .....	9
2.2.2 Soil erosion modelling .....	11
2.2.3 On-site Effects of Soil Erosion .....	14

2.2.4 Off-site Effects of Soil Erosion .....	14
2.3 Soils of Botswana.....	15
2.4 Characteristics of the Luvisols .....	15
2.5 Soil Properties .....	16
2.5.1 Soil Reaction (pH).....	16
2.5.2 Soil Organic Carbon (SOC).....	17
2.5.3 Cation Exchange Capacity (CEC) .....	18
2.6 Soil Nutrient Depletion .....	19
2.6.1 Acidification .....	19
2.7 Importance of Soil Fertility Management .....	20
2.8 Application of Remote Sensing (RS) and Geographical Information System (GIS).....	21
2.8.1 Change detection .....	21
2.8.2 Estimation of Spatial Rainfall Distribution .....	23
2.8.3 Satellite Image Processing and Analysis .....	24
2.8.4 Image Classification .....	24
2.8.5 Ground Truthing .....	25
2.8.6 Accuracy Assessment .....	25
CHAPTER 3: MATERIALS AND METHODS .....	26
3.1 Study Site Description.....	26
3.1.1 Geographical Location and Size.....	26
3.1.2 Climate.....	26
3.1.3 Soils .....	27
3.1.4 Topography.....	27
3.1.5 Vegetation.....	27
3.2 Methods of Data Collection and Processing .....	28
3.2.1 Land use land cover (LULC) determination.....	28
3.2.2 Image Classification Process .....	28

3.2.3 Accuracy Assessment .....	29
3.3 Assessment of Soil Fertility .....	30
3.4 Mapping of Soil Erosion Hazards .....	31
3.4.1 Rainfall Energy (E).....	31
3.4.2 Soil Erodibility Factor (F) .....	34
3.4.3 Slope Length and Slope Steepness .....	34
3.4.4 Topographic Factor (X) .....	34
3.4.5 Crop Ratio (C).....	35
3.4.6 Principal Factor (K) .....	35
3.5 Soil Loss Analysis .....	35
3.6 Software Packages and Data Processing .....	37
CHAPTER 4: RESULTS AND DISCUSSION.....	38
4.1 Land use land cover change (LULCC) detection.....	38
4.1.1 Image Classification .....	38
4.1.2 LULC change detection.....	39
4.1.3 LULC Change Analysis.....	39
4.1.4 Accuracy Assessment .....	41
4.2 Assessment of Soil Fertility .....	44
4.2.1 Baseline Data .....	44
4.2.2 Comparison of Soil Parameters before and after ISPAAD .....	48
4.3 Mapping of Soil Erosion Hazards .....	51
4.3.1 Topographic Ratio (X).....	51
4.3.2 Rainfall Energy (E).....	52
4.3.3 Soil Erodibility Factor (F) .....	52
4.3.4 Principal Factor (K) .....	52
4.3.5 Crop Ratio (C) Factor .....	53
4.3.6 Determination of SLEMSA model (Z).....	54

4.3.7 Potential Erosion Risk Analysis .....	55
CHAPTER 5: SUMMARY AND CONCLUSION. ....	57
RECOMMENDATIONS .....	59
REFERENCES .....	60
APPENDICES .....	70
Appendix 1: Interpretation of Kappa statistics.....	70
Appendix 2:Error Matrix Summary Table (2006 and 2020).....	70
Appendix 3: Bar chart depicting LULCC in percentage.....	71
Appendix 4: Vegetation map of the study area .....	72
Appendix 5: Study area soil fertility and soil type maps .....	73
Appendix 6; Various change detection techniques .....	74
Appendix 7: Average annual rainfall in mm (2000-2019) Mochudi station.....	75
Appendix 8: Average annual rainfall in mm (1995-2019) Olifantsdrift station .....	76
Appendix 9: Average annual rainfall in mm (1995-2019) Sikwane station .....	77

## **CHAPTER 1: INTRODUCTION**

### **1.1 Status of Food Security in Sub-Saharan Africa (SSA)**

Insufficient food production has become a major problem in most of developing countries. This is the central reason for food shortage in the region (Mkonda, 2017; SADC, 2016). Sub-Saharan Africa (SSA) is estimated to have 223 million people who are food insecure and undernourished (FAO et. al, 2013). Food security is believed to be core to human development and capability, and therefore, enhancing food availability and entitlements is a robust way to sustainable human development (Mkonda, 2017). Sub-Saharan African countries including Botswana are vulnerable to climate change due to their dependence on rain-fed agriculture (AGRA, 2014). Productivity of SSA agriculture depends on climate, efficient and effective use of factors of production (farmland, water and labour), agricultural inputs (fertilizers, irrigation, seeds and capital equipment) and farmers' skills.

The status of food insecurity in Southern Africa is also very high. Many countries in the region, save South Africa, are net importers of staple food due to low crop yields (FAO, 2010). The FAO (2010) report (REOSA, 2010) further states that more than 70 % of the population, and most of the poor, are engaged in smallholder rain-fed agriculture and related activities. Introduction of government's subsidies for supporting the smallholder farmers is one way of stimulating economic growth in the region and help the rural poor to combat poverty. Higher farm productivity and more diversified farm produce will reduce the need to buy supplementary foodstuffs, provide a healthier diet and offer the possibility of selling food surplus for cash.

Climate change has negatively impacted on food production for the rapidly growing population in SSA. Food production has not kept pace with population growth. More erratic weather patterns and extreme weather events contribute to low yields in the region (AGRA, 2014). The number of extreme events such as droughts, floods and hurricanes has increased in the recent years, as has the unpredictability of weather patterns, leading to substantial losses in production and lower incomes in vulnerable areas (FAO et al., 2013). The AGRA (2014) Report further mentions that the length of growing period (LGP) which is an indicator of the adequacy of moisture availability, temperature and soil conditions for crop growth is projected to decrease by up to 20 % for most parts of SSA (AGRA, 2014). This climatic

change badly affects the livelihood of smallholder arable farmers, pastoralists and poor consumers.

Recent studies suggest that late rains in Southern Africa may be due to changing weather patterns as a result of the El-Niño effect (FAO, and. GoB., 2016). The delays eventually impact on the type of farming systems adopted by farmers. The onset of the ploughing season in Botswana is normally from October to January. In the recent cropping seasons, most areas would have not received enough rainfall. As a result, very little ploughing (and planting) is normally done.

Many of the smallholder farmers use unsustainable management practises. They use farming methods which negatively impact on the soil. The soils for smallholder farmers in Southern Africa have been severely depleted through generations of unsuitable farming methods including ploughing, mono-cropping, little or no replenishment of nutrients and burning of residue (FAO, 2010). The poor and unsustainable management practices lead to land degradation and ultimately decreased crop yields.

Depleted soil nutrient status is the number one cause of low yields in Africa that leads to hunger and starvation (Amuri et al, 2010). The common fertilizers available in the market supplies only nitrogen (N), phosphorus (P), and potassium (K). This is because N, P, and K are the major essential nutrients, which are depleted at faster rate than other nutrients such as sulphur (S), calcium (Ca), magnesium (Mg) and micronutrients. It is possible that after long term cultivation other nutrients in addition to NPK may be depleted to the extent of limiting crop yields (Amuri et al, 2010).

Dinogeng is one of the major food crops' producing extension areas in the Kgatleng District supporting many of the rural poor people. The study area is situated in the eastern part of the country where the soils are comparatively fertile. However, these soils have been under cultivation for a long period of time and decline in soil fertility is very likely hence the need for soil testing and proper soil management for better yields.

## **1.2 Status of Traditional Arable Agriculture in Botswana**

Botswana is divided into nine Agricultural Districts and has a total land area of 582 000 km<sup>2</sup>. Each district is sub-divided into Agricultural Extension Areas. The country is sparsely populated with a population of a little over 2 million (Statistics Botswana, 2014). The country is characterized by semiarid climate with erratic rainfall that supports all agricultural

activities carried out to sustain livelihoods of many households. About 36 % of the population now live in rural areas and depend on agriculture for sustenance. Agriculture is an important sector in the economy of Botswana because it provides food, income and employment for the majority of the rural dwellers (Statistics Botswana, 2015). Agriculture has a potential for growth and creation of employment opportunities particularly for the unskilled and semi-skilled people. Poor performance of the arable sector has led to rapid population migration to urban areas. About 62 % of the nation lived in towns in 2010 compared to 60 % in 2008 (Statistics Botswana, 2014).

Botswana gained independence in 1966. Its agricultural sector contributed about 40 % to Gross Domestic Product (GDP) and by 2011 until present this value has decreased to about 2 % of the overall GDP (Statistics Botswana, 2014; World Bank Group, 2015). The decline was mainly attributed to the rapid increase in the contribution of minerals, particularly diamonds, to the country's GDP. Agriculture, however, remains a significant source of food, income and employment for majority of rural households (AGRA, 2014; Seleka, 1999).

While the decline in the relative contribution of agriculture to Botswana's economy is largely attributable to the discovery of minerals, other sources of this trend originate from within the sector itself (Seleka, 1999). The arable sub-sector has been characterized by low productivity levels, implying low returns to labour and capital investments. This poor performance has been largely attributable to low and variable rainfall and the occurrence of successive droughts (AGRA, 2014; BCA Consult, 2012; Seanama Conservation Consultancy, 2012). Arable sub-sector factors such as poor soil fertility, land degradation, low adoption of improved technologies, poor farm management, inadequate farm inputs, inadequate draft power at critical times and insufficient knowledge and training of both extension agents and farmers have also been advanced as plausible sources of low productivity levels (Seanama Conservation Consultancy, 2012; Seleka, 1999). The poor performance in the arable sub-sector has contributed to the country's dependence on imports to secure basic cereals which accounts for about 90 % (BCA Consult, 2012).

Governmental support to farmers has been substantial in an effort to increase arable production and productivity at national and farm levels. Various policies have been formulated and several programmes implemented to boost the arable sub-sector productivity (Ministry of Agriculture, 2013; Seleka, 1999). These programmes have been accompanied by huge government expenditure. Arable Land Development Programme (ALDEP) and the

Accelerated Rain-fed Arable Programme (ARAP) dominated the arable sub-sector since early to mid-1980s. Despite the government support, low and declining productivity continued to characterize the arable sub-sector (Ministry of Agriculture, 2013; Seleka, 1999). The challenges in the arable sub-sector led to the introduction of the Integrated Support Programme for Arable Agricultural Development (ISPAAD) (BCA Consult, 2012; FAO and GoB, 2016; Statistics Botswana, 2014). Furthermore, Government's support was also motivated by objectives to achieve household and national food security as well as social protection of farmers against agricultural risks, vulnerability and market failure (BCA Consult, 2012).

In Botswana, the total number of farmers was 31,000 in 2007/08 (before ISPAAD). The number of ISPAAD beneficiaries was 96,000 in 2008/09 when ISPAAD started. The number of beneficiaries increased to 118,000 in 2010/11. The area planted was 104,000 ha in 2007/08. The area planted increased to 298,000 ha in 2008/09 and rose to 377,000ha in 2010/11 (BCA Consult, 2012). The total domestic grain production during ISPAAD averaged 58,000 tons per year. Productivity remained low and continued to decline during ISPAAD (Statistics Botswana, 2015). The national average grain productivity was 320kg/ha of grains against an expected ISPAAD target yield of 1000kg/ha. Domestic grain production only satisfied about 10 % of national staple grain requirement. Botswana imported an average of 300,000 tons of cereal grains per year during ISPAAD (BCA Consult, 2012).

Dinogeng is situated in the Kgatleng district where intensive agriculture is practised. The district has a total land area of 7600 km<sup>2</sup>; 6.9 % of the area is used for arable farming, 13.6 % for mixed farming whilst 43.2 % is utilized for communal grazing (Kgatleng District Council, 2002). Dinogeng covers a land area of approximately 83 km<sup>2</sup>. According to the Ministry of Agriculture records, Dinogeng has more than 4000 arable farmers benefiting from ISPAAD programme each year.

### **1.3 Brief Description of ISPAAD Programme**

The primary objectives of ISPAAD are to increase grain production, promote food security at the household and national levels, commercialize through mechanization, and facilitate access to farm inputs and credit and to improve extension outreach (Ministry of Agriculture, 2013). The expected outcomes from ISPAAD include improvement of farm output and productivity through enhancement of farmers' access to inputs comprising seeds, fertilizers, draught power, credit, cluster fencing, potable water and other agricultural services.

According to ISPAAD guidelines, there is a general eligibility criterion used for farmers to benefit from the programme. All farmers aged 18 years and above with Omang or residence and work permit must produce proof of ownership or access to arable land. Farmers are required to register with the Extension Agent in their area. The ISPAAD beneficiaries also stand a chance of being blacklisted in the future if they do not take a good care of their arable land.

Farmers are provided with free seeds of open pollinated varieties of maize, sorghum, millet and cowpeas to plant a maximum of 16 ha. For more than 16 ha, farmers can source seeds from locally registered suppliers at 50 % subsidy. Hybrid and fodder crop seeds are also obtained at 50 % subsidy without any limitation in terms of area to be planted. Government provides free fertilizer up to a maximum of 5 ha at a rate of 200 kg/ha on condition that farmers row plant and have access to fertilizer applicators. Additional fertilizer up to a maximum of 11 ha is provided at 50 % subsidy. The ISPAAD also assists farmers with machinery and associated implements through Agricultural Service Centres or private contractors. Arable farmers are assisted to plough, harrow and row plant a maximum of 5 ha for free. In addition, farmers could be assisted to plough/harrow/row plant additional 11 ha at 50 % subsidy. All services as well as machinery and implements hired will be paid in advance at Government set prices outlined in the ISPAAD guidelines.

#### **1.4 Statement of the Problem**

Insufficient food production is a major problem in Botswana. Government introduced ISPAAD subsidy programme in 2008 to support arable farmers to increase arable production for achievement of household and national food security. The area of land planted and the number of ISPAAD beneficiaries increased when the programme was introduced but production remained low (BCA Consult, 2012). Most of the arable farmers are smallholder farmers who lack farming skills, resources and dependant on rain-fed agriculture which is vulnerable to climate change. The soils for smallholder farmers have been severely depleted through generations of unsuitable farming methods including ploughing, mono-cropping, little or no replenishment of nutrients and burning of residue (FAO, 2010). Use of unsustainable farming techniques has led to land degradation which can be revealed by poor yields. Therefore, the study seeks to assess soil erosion risk and soil fertility changes due to ISPAAD programme in Dinogeng Agricultural Extension Area (DAEA).

### **1.5 Significance of the Proposed Study**

Suitable land for arable farming is very scarce in Botswana and the hard veld in the eastern part of the country has been the focus of interest for several years because of comparatively fertile soils. The country is a net importer of food grains due to low crop yields (FAO, 2010). The causes of low crop production include unfavourable climate, poor soils and unsuitable farming methods leading to land degradation. With increasing population and failure to adopt agricultural technology by farmers, this may worsen the quality and quantity of agricultural land and its productivity in the long term.

Abandoning existing farmland and searching for new agricultural fields are likely to happen and this may translate into land use changes, land use conflicts and deforestation. To address some of these problems, there is need for a study on the assessment of the impacts of the ISPAAD programme on the environment in DAEA. Dinogeng has a considerably higher number of smallholder farmers benefiting from the ISPAAD programme each year, and so chances of land degradation are very high, hence the pressing need for this study.

The results of this study are going to be applicable to the whole country; for example, Geographical Information System (GIS) and Remote Sensing (RS) capabilities can be used to quantify and map potential erosion risk areas for effective land use and soil conservation planning in an affordable and timeous manner. According to Moesi (2021), Soil erosion models are useful for estimating soil loss and runoff rates at watershed and basin level, planning land management strategies, providing relative soil loss indices and guiding government policy and strategy on soil and water conservation practices. On the other hand, the findings for soil fertility analysis can provide useful information for development of soil fertility management strategies by government or decision makers.

### **1.6 Purpose of the Proposed Study**

The purpose of the study was to fill the existing knowledge and information gap about assessment of soil erosion risk and soil fertility changes before and after ISPAAD programme in Dinogeng Agricultural Extension Area in the Kgatleng District. The study specifically determined land use land cover changes (LULCC) using Geographical Information System (GIS) and Remote Sensing (RS) for the period from 2006 to 2020, analysed soil fertility for the period before and after inception of ISPAAD and mapped soil erosion hazard areas using the Soil Loss Estimation Model for Southern Africa (SLEMSA) and geospatial techniques.

### **1.7 Aim of the Study**

The main objective of this study was to assess soil erosion risk and soil fertility changes before and after ISPAAD programme using GIS and RS in Dinogeng Agricultural Extension Area.

#### **1.7.1 Specific Objectives of the Study**

The specific objectives of this study were:

1. To determine land use land cover changes (LULCC) using GIS and RS for the period from 2006 to 2020;
2. To analyse soil fertility changes for the period before and after inception of ISPAAD (1988 to period between 2009 and 2019);
3. To map out soil erosion risk using SLEMSA model and GIS.

## CHAPTER 2: LITERATURE REVIEW

### 2.1 Land use changes

Many researchers argue that land use land cover change (LULCC) emerged as a major aspect in the wider debate of global change; and that change originates from human-induced impacts on the environment and their implications for climate change (Cheruto et al, 2016). The indicators of these changes can be clearly seen in the current major global concerns such as increasing concentrations of carbon dioxide (CO<sub>2</sub>) in the atmosphere, loss of biological diversity, conversion and fragmentation of natural vegetation areas and accelerated emission of greenhouses gases.

Land use land cover change has been recognised as one of the major drivers for global environmental change resulting in land degradation (Schöber et al, 2010). On the regional scale, land use induced environmental changes, such as biodiversity loss, reduction of land productivity because of soil degradation, problems of land and water contamination, and the lowering of groundwater tables, can be intense (Schöber et al, 2010). Often regional-scale responses become evident more quickly than at the global scale. From an economic point of view land is an essential factor of production, and land productivity has been strongly tied to economic growth. However, land is more than only a production factor; it is a key finite resource for most human activities including agricultural production.

Land use change has important impacts on socioeconomic and environmental systems with important trade-offs for sustainability, food security, biodiversity, and the vulnerability of people and ecosystems to global change impacts (Hano, 2013). Land use land cover (LULC) plays a key role in sustainable development. In land use decision-making, sustainability impact assessment is essential and provides key information about impact pathway relationships based on complex scientific analysis (Schöber et al, 2010). Land use contributes widely to land degradation. Many studies have revealed that LULC and subsequent conversion have led to deterioration in the physical and chemical properties of soil, causing degradation of the land.

#### 2.1.1 Land-Use/Land-Cover Change

Land cover is a material that is found above the earth's surface such as vegetation, water, etc while Land use is what that material is being used for; examples include agriculture, settlement, etc (Moesi, 2021). Land use land cover (LULC) information is very crucial for modelling and understanding the earth's feature system. Vegetation cover such as forest,

shrub land and agricultural area has a massive effect on the soil loss process. The soil erosion rate is influenced by land use and cover practices such as deforestation, overstocking, overgrazing, and agricultural intensification on arable lands.

## **2.2 Land degradation**

Land degradation is a serious global concern since it diminishes the planet's capacity to provide food to the world at large (Hano, 2013). Land degradation is defined as the loss of the productive capacity of the land to sustain life. Soil erosion is one of the biggest global environmental hazards causing severe land degradation (Tiruneh and Ayalew, 2015). Population explosion, deforestation, unsustainable agricultural cultivation, and overgrazing are among the main factors causing soil erosion hazards. There is no single factor that causes land degradation, it is caused by a combination of factors that change over time and vary by location. The principal driver of human-caused land degradation is unsustainable exploitation of land by pastoral farming, arable cropping, and agro-pastoral land uses (Hano, 2013). According to Kayombo et. al. (2005), land degradation is prevalent throughout Botswana. Some studies have reported that land degradation in the country has resulted in low crop yields, poor livestock off-take, and low rural household incomes as a result of poor utilization of land resources (Tersteeg, 1993; Wingqvist and Dahlberg, 2008). According to Annepu et. al. (2017), land cultivation without best management practices leads to environmental degradation through loss of soil fertility and this may result in deforestation and decrease in agricultural land caused by demand for alternative land uses.

### **2.2.1 Soil erosion process and contributing factors**

Before modelling soil loss, it's important to understand the soil loss process, its contributing factors, its various forms, and the commonly used models. Soil loss is a negative environmental process that begins in the early stages as structural deterioration and advancing to overland flow and rill erosion, and finally to gully and riverbank erosion. Prevention and control of soil loss at the early stages is much easier and less expensive than at the late stages.

During soil loss, the soil particles are first detached then transported before being deposited some distance away from the initial position. Particle detachment occurs when the individual soil particles are broken off from the soil mass due to shearing force (e.g. from tillage equipment, hooves of animal, surface runoff, etc.) or due to impact force (e.g. from raindrop) on the soil. Rain splash is the most important detaching agent as a result of raindrops striking a bare soil surface (Morgan, 2005). The detachment forces are effective where the soil is vulnerable (easily detachable). Soil vulnerability is brought about by the inherent soil

properties (due to weak chemical and physical soil properties), continuous poor soil management, and prolonged exposure to the weathering actions (Vargas et al, 2016). The forces also produce maximum effect if there is minimal restrictive soil cover (such as vegetation cover, mulches, abandoned crop- residue on farm, etc.).

After detachment, the soil particles are moved away from their original place through a gradient (Vargas et al, 2016). The most common sources of energy for transport are surface runoff or wind. These forces carry the detached soil particles either in suspension or by dragging them along the soil surface. They transport the soil in a sheet of moving water/wind or in concentrated channels such as rills or gullies. Overland flow/rill/gully types of erosion derive their names from this aspect of soil loss transport. The transport energy, slope, and length of slope (for travel time) must be available for the transport phase of soil loss to be accomplished. Deposition usually occurs at the end of the transport phase when enough energy is no longer available to transport the particles.

The conceptual model or flow chart (Figure 2.1) illustrates the following basic contributing factors to soil loss (Vargas et al, 2016).The Soil Loss Estimation Model for Southern Africa (SLEMSA) input data includes rainfall, soil units, slopes and land cover:

- a) Soil Erodibility (vulnerability of the soils) -Soils with weak structure, shallow depth, and medium to fine texture.
- b) Rainfall Energy (detachment or transport energy) -It's also known as agents of erosion and comes in the form of rainfall, runoff, or wind energy. They initiate the erosion process and transport the detached particles.
- c) Land use land cover - It represents human intervention/acceleration in the erosion process as well as the vegetative cover to protect the soil against agents of erosion.
- d) Topographic factors– They include slope and slope length. They provide the gradient for translating the detached soil.

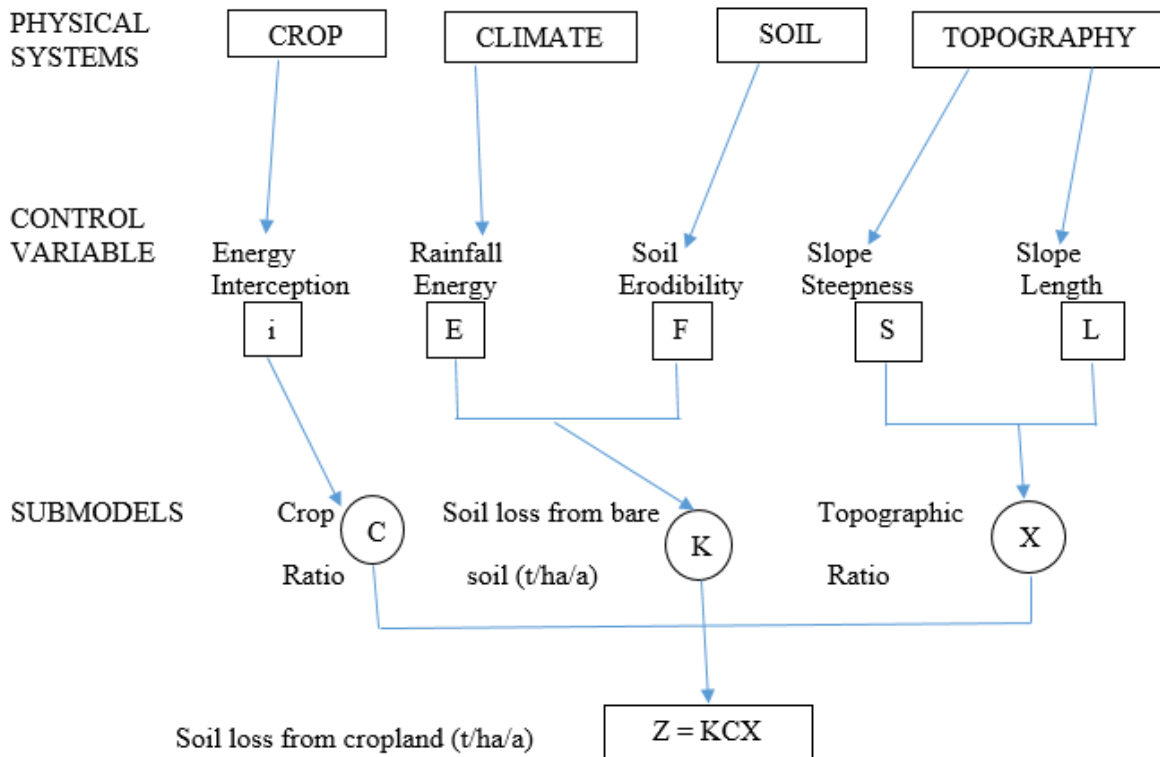


**Fig. 2.1. Framework for SLEMSA model**

### 2.2.2 Soil erosion modelling

Modelling soil erosion is the process of mathematically describing soil particle detachment, transport and deposition on land surfaces. Erosion models can be used as predictive tools for assessing soil loss, conservation planning, soil erosion inventories and project planning (Bobe, 2004). Moreover, they can be used as tools for understanding erosion processes and their impacts.

A variety of approaches and models were developed to assess soil erosion by water and to predict soil erosion risk and intensity. Each approach or model has its own characteristics and purpose of application. Available quantitative and semi-quantitative models for predicting soil erosion at a basin scale were reviewed and evaluated in detail. Among the commonly used empirical erosion models include: the Universal Soil Loss Equation (USLE) (Wischmeier and Smith., 1978), the Revised Universal Soil Loss Equation (RUSLE) (Renard et al, 1994) and SLEMSA (Elwell, 1978). Physical-based models namely the European Soil Erosion Model (EUROSEM) and the Chemicals, Runoff, and Erosion from Agricultural Management Systems (CREAMS) were developed for soil erosion and sediment transport (Morgan et al., 1992; Lane et al., 1992). These models were recently reviewed and discussed (Merritt et al., 2003) in terms of their structure, the scale of their intended use, assumptions

and capabilities, simulation of catchment processes, model input data and output results, predictive accuracy and limitations, and hardware requirements of the model.

### **2.2.2.1 Model selection**

In Africa, particularly Southern Africa, there are two popular models used: the Revised Universal Soil Loss Equation (RUSLE) and Soil Loss Estimation Model for Southern Africa (SLEMSA)(Vargas et al, 2016). The Universal Soil Loss Equation (USLE) by Wischmeier and Smith (1978) is a widely used soil loss model worldwide. The dominant model adopted in most countries in Southern Africa and selected for this study is the SLEMSA model. According to Stocking et. al. (1988), SLEMSA was initially developed mainly from data from Zimbabwe, to assess the erosion hazard that resulted from diverse farming systems that could promulgate proper recommendations for conservation measures. The SLEMSA model is based on a blend of factorial scoring methods and empirical relations with drivers of erosion. The SLEMSA model is essentially a model for soil removal (Schulze, 1979). It can be regarded as a useful model for differentiating areas of high and low erosion potential (Schulze, 1979; Smith, 1999). This was confirmed in the application of the Soil Water Erosion Assessment Program (SWEAP) model to the SOTER (soil and terrain) database at a scale of 1: 1 000 000 (Schulze, 1979). The SLEMSA was developed in Southern Africa based on the USLE and was an attempt to adapt the USLE model to an African environment. Introduction of Geographical Information Systems (GIS) and Remote Sensing (RS) technology has made it possible to implement the equation in a spatially distributed manner. Within a raster-based GIS, prediction of soil erosion on a cell-by-cell basis using the SLEMSA model is viable. This is particularly beneficial in the attempted identification of the spatial patterns of soil loss that are within a large region. Subsequently, GIS can be applied in the isolation and query of these locations to produce information essential to the role of individual variables contributing to the observed erosion potential.

Through the SLEMSA model, the soil erosion environment has been categorized into four physical systems, namely land cover, climate, soil and topography (Elwell, 1978). The design of the model is like that of USLE, the only difference being the method of combining the inputs. The USLE assigns the same weight to all inputs, whilst SLEMSA assigns more weight to the crop factor. Estimation of the erosion risk with SLEMSA requires that an initial erosion hazard index (K), which incorporates rainfall energy (E) and the soil erodibility class (F) be calculated first. The definition of K is the erosion hazard for bare soil at a 4.5 % slope of 30m long with potential exponential increase related to increasing rainfall energy and

increasing soil erodibility. Calculation of the final erosion hazard index is conducted through the multiplication of K by a cover factor (C) and a topography factor (X).

The SLEMSA is a relatively widely used soil loss model in African environments (Elwell and Stocking 1982). The SLEMSA model has been used to predict soil losses from small-scale farming and mining areas in Zimbabwe (Grohs and Elwell, 1993) and South Africa (Bvindi, 2019). The model has also found application in the development of erosion hazard map for the SADC region (Stocking et al., 1988; Le Roux., 2005), and for assessing areas of high silt discharge in South Africa (Schulze, 1979). Furthermore, SLEMSA has found use in modelling soil erosion in Zimbabwe (Dube, 2011), Botswana (Abel. and Stocking, 1987), South Africa (Breetzke et.al, 2013), Ethiopia (Bobe, 2004), Nigeria (Igwe, et. al, 1999) and Malawi (Paris, 1990). The details of the descriptions of the input factors considered, their assumptions, and procedures of the SLEMSA model are presented in Chapter 3.

#### **2.2.2.2 Strengths of the SLEMSA model**

SLEMSA is useful in estimating soil loss rates from agricultural land, in planning land use strategies and soil conservation, in providing relative soil loss indices and for guiding government policy and strategy on soil and water conservation (Vargas et al, 2016). Since model parameters are empirically derived, they are simple and parsimonious, and their input data can be relatively obtained from meteorology departments, and land survey and soil departments. Furthermore, the data, pre-processing models, and the soil loss model applications can be easily implemented in many freely downloadable GIS and database software. This makes SLEMSA model easily adaptable for application in many regions of the world.

#### **2.2.2.3 Limitations of the SLEMSA model**

The SLEMSA model has several limitations outlined as follows:

- 1) According to Stocking et al. (1988), the main limitation of the SLEMSA model is that it assumes that each factor in erosion has equal weight and importance, which is not true because, for instance, erosion rates are far more sensitive to changes in vegetation than to changes in soil type under tropical conditions (Bvindi, 2019).
- 2) The model technique uses the ordinal or ranking scale of measurement where erosion is implicitly linearly related to the rank of the variable. This ignores, for example, the important exponential relationship between vegetation cover and erosion (Elwell and

Stocking, 1976), meaning that a change in cover from 10 to 20% is proportionately far more effective in reducing erosion than a change from 70 to 80%.

- 3) SLEMSA assumes that erosion hazard is the multiplying effect of each variable, ignoring known complex interactions.
- 4) The model is based on statistical analyses of important factors in the soil erosion process and yield only approximate and probable outcomes (Vargas et al. 2016). It is also not practical for the prediction of soil loss on an event basis. The model estimates soil erosion on a single slope instead of within catchments. It also does not represent the process of sedimentation or deposition and is restricted to sheet and/or rill erosion. Furthermore, the model does not account for off-site effects of erosion.

### **2.2.3 On-site Effects of Soil Erosion**

On-site effects are particularly important on agricultural land where the redistribution of soil within a field, the loss of soil from a field, the breakdown of soil structure and the decline in organic matter and nutrient result in a reduction of cultivable soil depth and a decline in soil fertility (Morgan, 2005). Erosion also reduces available soil moisture, resulting in more drought-prone conditions. The net effect is a loss of productivity, which restricts what can be grown and results in increased expenditure on fertilizers to maintain yields. If fertilizers were used to compensate for loss of fertility arising from erosion in Zimbabwe, the cost would be equivalent to US\$1500 million per year according to Stocking (1986), which is a substantial hidden cost to that country's economy. The loss of soil fertility through erosion ultimately leads to the abandonment of land, with consequences for food production and food security and a substantial decline in land value.

### **2.2.4 Off-site Effects of Soil Erosion**

Off-site problems arise from sedimentation downstream or downwind, which reduces the capacity of rivers and drainage ditches, enhances the risk of flooding, blocks irrigation canals and shortens the design life of reservoirs. Many hydroelectric and irrigation projects have been ruined because of erosion. Sediment is also a pollutant and, through the chemicals adsorbed to it, can increase the levels of nitrogen and phosphorus in water bodies and result in eutrophication. Erosion leads to the breakdown of soil aggregates and clods into their primary particles of clay, silt and sand. Through this process, the carbon that is held within the clays and the soil organic content is released into the atmosphere as CO<sub>2</sub>. Lal (1995) has estimated that global soil erosion releases 1.14PgC annually to the atmosphere. Erosion is

therefore a contributor to climatic change, since increasing the carbon dioxide content of the atmosphere enhances the greenhouse effect.

### **2.3 Soils of Botswana**

The soils of Botswana were mapped under the Soil Mapping and Advisory Services Project of FAO/UNDP on a reconnaissance scale (Joshua, 1991). Most of the soil profiles which were described were sampled and characterized according to their chemical properties. The measurements of physical properties were limited to some selected profiles because they both required field and laboratory work and its time consuming. The physical properties measured include: Particle size distribution, bulk density, infiltration characteristics, moisture retention and structural stability of surface soil. The results obtained were stored in a computer for retrieval and interpretation.

Particle size distribution, bulk density and structural stability are specific to each soil therefore they need to be measured directly (Joshua, 1991). Infiltration and moisture retention are dependent to a large extent on the texture of the soil. However, these properties are often modified by pore size distribution, bulk density and structural stability and other site-specific conditions such as faunal activity and land use. Reliable estimates of infiltration and moisture retention properties are also obtained by direct measurement of soil. On the other hand, available moisture for plant growth can be derived from moisture retention properties using regression equation.

It has been reported that vegetation does not have a strong influence on the formation of soils in Botswana because of the climatic conditions (Rammelzwaal, 1989). The production of organic matter may be relatively high but very little is added into the soil due to high oxidation under the present condition. It is only under wet condition that the level of organic matter may be substantially higher. The levels of organic matter are usually found higher on calcareous materials.

### **2.4 Characteristics of the Luvisols**

By definition, the luvisols have a moderate to high base status and do not have major constraints regarding acidity, calcium deficiency and phosphate fixation (FAO, 1984). Luvisols straddle the sub-humid and the semi-arid zones. Sub-humid luvisols occur on strongly weathered parent materials; clay fraction is of low activity hence the total amount of plant nutrients is still low and major elements are deficient. Semiarid luvisols develop from a variety of parent materials; generally, less strongly weathered which determine their chemical

composition. The saturated complex is dominated mostly by calcium, as a result of which deficiencies of microelements such as zinc may occur. Major constraints include moisture stress and sensitivity to erosion when there is no crop cover. Low aggregate stability and surface sealing by rains, resulting in increased runoff and impeded plant germination are also common in Luvisols.

## **2.5 Soil Properties**

Soil physical, chemical and biological properties affect many processes in the soil that make it suitable for agriculture and other purposes (McCauley et al., 2005). Texture, structure, and porosity influence the movement and retention of water, air and solutes in the soil, which subsequently affect plant growth and organism activity. Most soil chemical properties are associated with the colloid fraction and affect nutrient availability, biota growing conditions, and, in some cases, soil physical properties. Biological properties in soil contribute to soil aggregation, structure and porosity, as well as soil organic matter (SOM) decomposition and mineralization. Organism activity is controlled by various soil conditions and may be altered by management practices. Since many soil properties are interrelated with one another, it is difficult to draw distinct lines of division where one type of property dominates the behaviour of the soil. Therefore, understanding and recognizing soil properties and their relationships is important for making sound decisions regarding soil use and management.

### **2.5.1 Soil Reaction (pH)**

The soil pH is the negative logarithm of the active hydrogen ion ( $H^+$ ) concentration in the soil solution. It is the measure of soil acidity or alkalinity. The pH of a soil is among the most important soil characteristics for crop production (Kettering et al., 2005). A soil with a pH value of 7 or greater is called an alkaline or basic soil. If the pH is less than 7, the soil is said to be acidic. Soil pH is a simple but very important estimation for soils as it has a considerable influence on the availability of nutrients to crops. It also affects microbial population in soils. Most nutrient elements are available in the pH range of 5.5 – 6.5 (FAO, 2008).

As soils become increasingly acidic, important nutrients like phosphorus become less available to plants (Kettering et al., 2005; USDA, 1998). Soil acidity affects the mobilization and availability of major nutrients such as nitrogen (N), phosphorus (P), sulphur (S), and basic cations (calcium (Ca), magnesium (Mg) and potassium (K)). It also regulates the rate of organic matter mineralization, reducing the number of simple organic molecules available for further decomposition and eventually rendering N and other constituent elements (P and S)

soluble (Vargas et al, 2016). Other elements, like aluminium, become more available and may actually become toxic to the plant, resulting in reduced crop yields (FAO., 2015; Vargas and Omuto, 2016). Liming to optimum pH not only increases the availability of essential nutrients, but also supplies additional calcium and magnesium, improves soil conditions for microorganisms, increases the effectiveness of triazine herbicides, and improves soil structure.

Human activity can change the pH of a soil through addition of most nitrogen fertilizers and organic nutrient sources such as compost and manure leading to formation of nitric acid ( $\text{HNO}_3$ ) and/or sulfuric acid ( $\text{H}_2\text{SO}_4$ ). Both are strong acids that cause an increase in soil acidity. It is therefore very important to test soil to determine if the pH is within the desired range. If a desirable pH is not maintained, then expected yields cannot be realized. Extra fertilizer cannot also fix a problem caused by low pH (Ketteringset. al, 2005).

### **2.5.2 Soil Organic Carbon (SOC)**

Soil Organic Carbon (SOC) is an important indicator of soil quality and well-known source of N, P and S in the soil (Omuto and Vargas, 2018). Besides holding positively charged  $\text{K}^+$ ,  $\text{Ca}^{2+}$ , and  $\text{Mg}^{2+}$  ions in the soil, SOC provides natural chelates that maintain micronutrients such as zinc, copper, and manganese in the forms that plants can use. Furthermore, the growth-promoting substances produced during organic matter (OM) decomposition and the structure it gives to soil tilth help the plant develop a more extensive root system, allowing it to obtain nutrients from a larger volume of soil. Soil organic carbon is globally recognized as the largest store of terrestrial carbon and a major player in climate change factors.

According to Gray et. al. (2016), SOC is influenced by factors such as climate, topography, parent material, soil fauna, and land use practices (Omuto and Vargas, 2018). Soil fauna and land use practices are within the control of a farmer to impact on the soil carbon pools at the farm level. A study by Lal (2018) and Ross (1993) observed that farming tends to mine the soil for nutrients and to reduce soil organic matter (SOM) levels through repetitive cultivation of soils, harvesting of crops and inadequate efforts to replenish nutrients and restore soil quality. A long term research by Maida and Chilima (1976) in Malawi has shown that 5 to 10 years of continuous cultivation can reduce the SOC content by as much as 40%. It is therefore expected that the decline in SOC in the cropland areas may be due to the unsustainable farming activities. This reinforces the recommendations or suggestions of

certain researchers that fertility problems may be solved through the use of integrated soil fertility management (FAO, 1984; Kavitha and Sujatha, 2015; Omuto and Vargas., 2018).

Although temperature is taken as a major control of SOM storage in SOC cycle models, temperature sensitivity to decomposition for different SOM fractions remains an area of uncertainty (FAO, 2015). Water also influences SOC storage through several processes. Moist but well-aerated soils are optimal for microbial activity. Decomposition rates consequently decrease as soils become drier. However, flooded soils have lower rates of SOM decay due to restricted aeration and thus may often yield soils with very high amounts of SOC (e.g. peat and muck soils). High precipitation may also lead to SOC transport down the soil profile as dissolved and/or particulate SOM. During extreme events, such as drought, SOM decomposition may initially decrease but may subsequently increase after rewetting.

The quantity and composition of SOC in mineral soils is also strongly dependent on soil type, with clay content influencing not only the amount but also the composition of SOC. According to Rumpel and Kögel-Knabner (2011), clay rich soils have higher SOM content and a higher concentration of O-alkyl carbon derived from polysaccharides may be expected, compared to sandy soils which are characterised by lower SOC contents and high concentrations of alkyl carbon (FAO., 2015). Aliphatic material may contribute to the hydrophobicity of soils, which could lead to reduced microbial accessibility and therefore increased SOC storage.

#### **2.5.2.1 Estimation of soil organic matter (SOM) from soil organic carbon (SOC)**

Soil organic matter is difficult to measure directly, so laboratories tend to measure soil organic carbon and use a conversion factor to estimate how much organic matter is held within a soil (Hoyle, 2013). About 58% of the mass of organic matter exists as carbon. Estimation of the percentage of SOM from the SOC% can be done using the conversion factor 1.72 derived from 100/58. This conversion factor can vary in different soils, but 1.72 provides a reasonable estimate of SOM for most purposes. The two parameters (SOM and SOC) are related in an equation as follows:

$$\text{Organic matter (\%)} = \text{total organic carbon (\%)} \times 1.72$$

#### **2.5.3 Cation Exchange Capacity (CEC)**

Cation exchange capacity is defined as a soil's total quantity of negative surface charges (Culman et. al, n.d.). The CEC of a soil is an important component of fertility derived from clay and organic matter content (Kayombo et. al, 2005). This is the capacity of the soil to

exchange nutrients with the soil solution. Cation exchange capacity is measured commonly in commercial soil testing labs by summing cations (Culmanet. al, n.d.). Soil CEC is a fundamental soil property used to predict plant nutrient availability and retention in the soil. It is the potential of available nutrient supply, not a direct measurement of available nutrients. The CEC typically increases as clay content and organic matter increase because cation exchange occurs on surfaces of clay minerals, organic matter, and roots.

In slightly acidic to neutral soils, calcium and magnesium take up approximately 80% of the CEC, while potassium only occupies less than 5% (OSU, 2004). In acidic soils, aluminium and hydrogen can begin to occupy a larger percentage of the CEC. The CEC of a soil depends largely on the soil texture and the amount of organic matter present. The larger the CEC value, the more cations the soil is capable of adsorbing, which decreases leaching. Attempts to increase the CEC of a soil by adding clay or organic matter are impractical due to the large amounts that would be necessary to affect a change. Liming acidic soils only affects the CEC slightly.

## **2.6 Soil Nutrient Depletion**

Nearly 3.3 % of agricultural Gross Domestic Product (GDP) in Sub-Saharan Africa is lost annually due to soil nutrient losses. Harvesting grains and crop residues from the land removes considerable quantities of SOC content. As lost nutrients in SSA are only very partially replaced with fertilizers, these losses contribute to negative nutrient balances (FAO, 2015). As a result, soil fertility decline has been described as the single most important constraint on food production and food security in SSA. Soil fertility decline (also described as soil productivity decline) is a deterioration of chemical, physical and biological soil properties. Besides soil erosion, the main processes contributing to nutrient depletion in SSA are: decline in organic matter and soil biological activity, degradation of soil structure and loss of other soil physical qualities, reduction in availability of major nutrients (N, P, and K) and micro-nutrients, and increase in toxicity, due to acidification or pollution.

### **2.6.1 Acidification**

Soil acidification is defined as a decrease in soil pH and is commonly a slow process under natural conditions (Guo et al, 2010). However, this process can be increased by a sequence of factors, including acidic precipitation and deposition of acidifying gases or particles, consequently resulting in a variety of environmental impacts. According to (Liu et al, 2018), soil pH values could be considerably changed within decades due to the influence of human activities. For example, acidification can be speeded by the application of nitrogen fertilizer,

which produces an excess of  $H^+$  ions in soil. It could also result from waste water percolating through the soil, which encourages the dissolution of soil carbonates. Possible cause of acidification according to (Jones and Olson-Rutz, 2020) includes;

- a) application of nitrogen fertilizer,
- b) No-till concentrates acidity
- c) availability of Soils with high sand content and/or low levels of soil organic matter
- d) Crop residue removal of base' cations (Ca, Mg, K)
- e) Leaching; Nitrate from fertilizer nitrification that is not taken up by plants but lost to leaching leaves  $H^+$  in the soil of these cations
- f) Legumes acidify their root-zone through N-fixation

## **2.7 Importance of Soil Fertility Management**

Soil fertility fluctuates throughout the growing season each year due to alteration in the quantity and availability of mineral nutrients by the addition of fertilizers, manure, compost, mulch, and lime in addition to leaching. Hence, evaluation of fertility status of the soils of an area or a region is an important aspect in the context of sustainable agriculture. Soil testing assesses the impacts of fertilizer application and provides recommendations on optimal rates for the soil year after year (Kavitha and Sujatha, 2015; Omuto and Vargas, 2018). According to FAO (2008), retesting of soils at least every four years to monitor soil fertility levels and pH to prevent nutrient deficiencies and excessive accumulation is required in most fields except for sandy and loamy sandy soils which require testing every two years.

The site-specific nutrient management practices reduce the cost of cultivation and environmental pollution due to the imbalanced application of chemical fertilizers. For proper soil management, the farmer should know what amendments are necessary to optimize the productivity of soil for specific crops (Annepu et. al., 2017; Kavitha and Sujatha, 2015). Management practices need to be implemented that sustain, restore or increase soil fertility and biomass production while limiting associated negative impacts (FAO, 2015). This can be achieved by promoting the accrual of SOM and nutrient recycling, applying balanced carbon amendments and fertilization of N, P and other nutrients to meet plant and soil requirements, while limiting overuse of fertilizer.

## **2.8 Application of Remote Sensing (RS) and Geographical Information System (GIS)**

Over the last decades, RS has proven to be a valuable tool for identifying objects at the earth's surface and for measuring and monitoring the spatiotemporal dimension of important biophysical characteristics and human activities on the terrain (Hano, 2013). Remote sensing plays an important role in a wide range of environmental disciplines, such as geography, geology, zoology, agriculture, forestry, botany, meteorology, oceanography, and civil engineering. According to Deb and Nathr (2012), LULC has become a crucial item or basic tasks in carrying out important works, such as the prediction of land-use change, prevention of natural disasters, management and planning of land uses, protection of environment, etc.,. Since the 1970s, RS has proved to be advantageous in providing dynamical, multi-temporal time series land cover information. Remote Sensing has been applied widely in dry land research, including assessment of land use changes and land degradation.

The integration of RS and GIS in environmental monitoring has become increasingly common in recent years. RS imagery is an important data source for environmental GIS applications, and conversely GIS capabilities are being used to improve image analysis procedures (Cheruto et al., 2016; Hano, 2013). Satellite RS is the only available means for systematic measurements of spatiotemporal surface parameters over large areas in a reproducible manner and at frequent rates. Remote sensing has long been recommended for its potential to detect, map, and monitor degradation with high spatial and spectral resolution and for the detection of degraded areas, including their dynamics of spread in time. Therefore, RS can serve as a means for the monitoring of spatial and temporal land degradation.

While it is true that decision makers need current techniques of geospatial information for planning processes, pattern and trends of land use and land cover change in rural Africa show little attention in terms of combining satellite images and other land use maps. Application of geo-spatial methods for land use and land cover dynamics is very scarce despite its relevance. Detailed information on land use and land cover changes with accurate statistics are not readily available in most tropical countries (Appiah et. al., 2017).

### **2.8.1 Change detection**

The surface of the earth changes endlessly due to the natural phenomena or human actions and the process of identifying the changes which has occurred over time on the earth surface is referred to as change detection (Mishra et al, 2017). Change detection of earth's surface is carried out effectively in the field of remote sensing using various techniques. The changes

on the surface of the earth occurs due to disasters, deforestation, change in course of river, urbanization etc. The earth's surface changes are divided into two categories which are land use and land cover. Change detection process can be done by traditional methods and by using remote sensing technologies. In this study, the traditional method was avoided because it's expensive, time consuming and not so accurate whereas all these problems are no existent with remote sensing technology.

### **Post classification**

This technique involves comparison of independently produced classified images. The approach of this method is based on the rectification of the classified images independently. Thematic maps are generated then followed by comparison of the corresponding labels to identify the areas where change has occurred. There are several advantages associated with this technique i.e. it minimizes sensor, atmospheric and environmental differences. Data from two dates are separately classified thereby minimizing the problem of normalizing for atmospheric and sensor differences between two dates.

### **Image differencing**

In this method, DN values of two spatially registered imageries which are acquired at different times are subtracted pixel by pixel and band by band. The difference between the DN values is calculated by using the formula:

$$DX_{ij}^k = X_{ij}^k(T_2) - X_{ij}^k(T_1)$$

Where  $X_{ij}^k(T_1)$  and  $X_{ij}^k(T_2)$  is the DN value of pixel X located at row i and column j for and k at time  $T_1$  and  $T_2$ .

If the difference between the DN values is 0, it represents no change. If the change occurs, the values are either positive or negative. In image differencing method, sometimes differences may occur even when the change has not occurred due to the reason that the exact registration of images and perfect radiometric conditions are never obtained for images which have been acquired at different dates.

Various change detection techniques and their suitability for detection of change are presented in tabular form (Appendix 6)

### **2.8.2 Estimation of Spatial Rainfall Distribution**

Rainfall is a highly significant piece of hydrologic data. The data is normally recorded as observational data through systematically planned rainfall station networks. However, rainfall records are often incomplete because of missing rainfall data in the measured period, or insufficient rainfall stations in the study area. To resolve the problems of such partial rainfall data, probable rainfall data can be estimated through spatial interpolation techniques (Chen & Liu, 2014).

Various spatial interpolation techniques have already been used in related fields. Such techniques can be divided into geographical statistics and non-geographical statistics. Examples include nearest neighbour, Thiessen polygons, splines and local trend surfaces, global polynomial, local polynomial, trend surface analysis, radial basic function, inverse distance weighting (IDW), and geographically weighted regression, which are all classified as non-geographical statistics. On the other hand, various forms of Kriging method are classified as geographical statistics.

Through IDW, the spatial rainfall field can be obtained when data over a whole catchment are interpolated. When using such method, the results have proven to be satisfactory as the stimulated data at individual sites preserved properties which mimicked the observed statistics at an acceptable level for practical purposes (Chen and Liu, 2014).

Different interpolation methods such as the combining stepwise regression and IDW, kriging, spline, and trend were tested. The result demonstrated that the combination of stepwise regression and IDW showed the highest accuracy in prediction, and was better than other methods. The study by Chen and Liu (2014) in Taiwan observed that the use of a radius of influence of up to 30 km in IDW interpolation technique provides optimum spatial rainfall estimates. In comparison, each method has its advantages and disadvantages based on its objectives, and hence the optimal interpolation method to be adopted varies for different purposes. In general, the advantage of the IDW method is its usefulness when the distribution of the estimated parameters is not a normal distribution.

#### **2.8.2.1 Inverse Distance Weighting (IDW)**

Inverse distance weighting is based on the concept of Tobler's first law of geography from 1970. It was defined as everything is related to everything else, but near things are more related than distant things. The IDW was developed by the United States National Weather Service in 1972 and is classified as a deterministic method. This is due to the lack of

requirement in the calculation to meet specific statistical assumptions. The IDW is thus different from stochastic methods such as Kriging (Chen and Liu, 2014).

The IDW technique is also used for multivariate interpolation. Its general idea is based on the assumption that the attribute value of an un-sampled point is the weighted average of known values within the neighbourhood. This involves the process of assigning values to unknown points by using values from a scattered set of known points. The value at the unknown point is a weighted sum of the values of known points.

### **2.8.3 Satellite Image Processing and Analysis**

The satellite image processing and analysis refers to the act of examining images for the purpose of detecting, identifying, classifying, measuring and evaluating the significance of physical and cultural objects, their patterns and spatial relationship. The image processing can broadly be categorized into: pre-processing, image classification or segmentation, post processing and evaluation. Detailed image processing procedures are available according to Campbell and Wynne (2011), Cheruto et al.(2016) and PCI Geomatics (2018).

Common pre-processing techniques include: Radiometric and geometric correction, Radiometric enhancement, Spatial enhancement, Spectral enhancement, and Fourier analysis. Radiometric correction addresses variations in the pixel intensities that are not caused by the object or scene being scanned. Several algorithms have been developed to radiometric correction. Since spatially varying haze is a common feature of archival Landsat TM scenes, which can affect the image classification quality, a pre-processing step to haze reduction is required.

### **2.8.4 Image Classification**

Image classification is the process of sorting pixels into a finite number of individual classes, or categories, of data based on their pixel values (Parece et al., 2011). If a pixel satisfies a certain set of criteria, then the pixel is assigned to the class that corresponds to that criterion. The classification process breaks down into two parts: training and classifying. Training is the process of defining the criteria by which these patterns are recognized. Training can be performed with either an unsupervised or supervised method (Campbell. and Wynne, 2011; Eastman, 2006).

#### **2.8.4.1 Unsupervised Classification**

Unsupervised classification is a method of identifying, grouping, and labelling features in an image according to their spectral values (Parece et al., 2011). The pixels are clustered

together based on spectral homogeneity and spectral distance. An analyst may choose from a variety of techniques to measure distances. One of the limitations is that unsupervised classification produces classes of homogeneous spectral identities that may not always correspond to informational classes.

#### **2.8.4.2 Supervised Classification**

In this process, pixels that represent recognizable patterns are identified and with the help from other sources are selected (Parece et al., 2011; PCI Geomatics., 2018). Knowledge of the data, the classes desired, and the algorithm to be used is required before selecting training samples. Patterns in the imagery are identified and the computer system is trained to identify pixels with similar characteristics. By setting priorities for these classes, the analyst supervises the classification of pixels as they are assigned to class values. Most researchers prefer supervised classification because it generally gives more accurate class definitions and higher accuracy than unsupervised approaches (Hano, 2013). If the classification is accurate, then each resulting class corresponds to a pattern that was originally identified.

#### **2.8.5 Ground Truthing**

The location of a specific characteristic, such as a land cover type, may be known through ground truthing. Ground truthing as described by Lillesand et al. (2015) is the attainment of knowledge about the study area from field work analysis, aerial photography, or personal experience.

#### **2.8.6 Accuracy Assessment**

In a statistical context, accuracy comprises bias and precision and the distinction between the two is sometimes important as one may be traded for the other. In thematic mapping from remotely sensed data, the term accuracy is used typically to express the degree of correctness of a map or classification. Parece et al. (2011) described accuracy assessment as a process that compares a classified image to an image which is assumed to be correct (such as an aerial photo, high resolution image of Google earth and Google Map, etc.). A thematic map derived from a classification may be considered accurate if it provides an unbiased representation of the land cover of the region it portrays. In essence, therefore, classification accuracy is typically taken to mean the degree to which the derived image classification agrees with reality or conforms to the truth (Agidewand Singh, 2017). An error matrix is considered the most common method of assessing the degree of accuracy and has been used widely in the classification accuracy assessment (Hano, 2013).

## CHAPTER 3: MATERIALS AND METHODS

### 3.1 Study Site Description

#### 3.1.1 Geographical Location and Size

The study was conducted in Dinogeng Agricultural Extension Area (DAEA). It extends from  $24^{\circ} 8' 0''$  to  $24^{\circ} 35' 0''$  S latitude and  $26^{\circ} 5' 0''$  to  $26^{\circ} 35' 0''$  E longitude and it covers an area of about 83 100 hectares. An overview of the boundary of the study area is given in Figure 3.1.

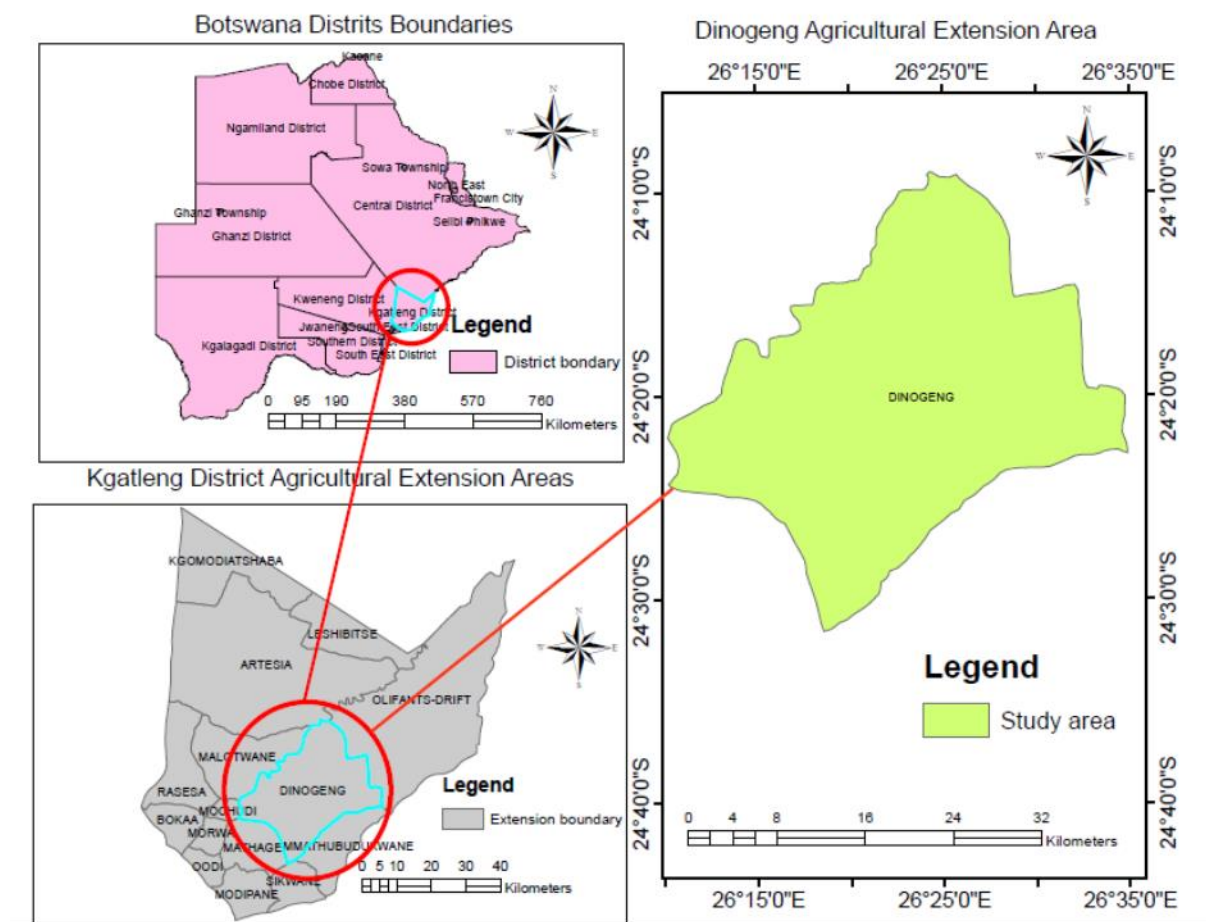


**Fig.3. 1 Location of the study area**

#### 3.1.2 Climate

The area of study is characterized by low and unreliable rainfall and very high summer temperatures. The climate is semiarid with a mean annual average temperature of  $20.7^{\circ}\text{C}$  fluctuating from  $13.2^{\circ}\text{C}$  to  $28.2^{\circ}\text{C}$  (Statistics Botswana., 2016). The semi-arid climate is characterized by erratic and high intensity rainfall. The annual precipitation of Dinogeng is based on the estimates obtained from the records of three nearby rainfall stations. The rainfall ranges from 348 mm to 404 mm with an average of 375 mm and standard deviation of 11

mm. The area receives summer rains and the rainy season is from the beginning of October to the end of March.

### **3.1.3 Soils**

The soils of Dinogeng area are predominantly Luvisols. These types of soils are characterized by a subsurface horizon of clay accumulation (an argillic B-horizon), a very high water retention capacity and nutrient status (Chanda, et al., 1999). The Kgatleng District Council (2002) described the soils in terms of the land unit system. The Notwane plain system straddles the Notwane River and comprises of soils that are deep light textured and acidic. The dominant soils have been reported to be sandy clay loam to sandy clay (BCA Consult, 2012). The soils are relatively poor but more fertile in comparison with the sandveld in the western part of the country. Soil fertility and soil type maps for the area of study are presented in Appendix 5.

### **3.1.4 Topography**

Dinogeng generally has flat and undulating topography with occasional rocky outcrops and several extensive drainage channel systems. The altitude of the area ranges between 901 m and 1003 m. There are neither hills nor permanent water bodies in the study area. The communities around Dinogeng depend on ground water for their livelihood. The drainage systems of Kgatleng district include the Notwane River which flows from south-west to north-east and streams that flow into the Notwane River until it reaches the Limpopo River.

### **3.1.5 Vegetation**

The vegetation map of Dinogeng presented in appendix 4 was clipped using GIS software from Kgatleng vegetation Map, shows that the area is dominated by shrubs with areas of woodland and savanna. Almost 50% of the area is covered by shrubs; about 7% is evergreen forest mainly along the Notwane River and other drainage lines within the study area. Tshireletso et al. (2018) revealed that, Kgatleng District lies within the woodland and thorn bush savanna ecosystems. Human related influences like unsustainable use of fuel wood and other activities, has changed the vegetation patterns considerably since the last century (Kgatlang District Council., 2002). Climate change also contributes significantly to the existing stresses causing changes in prevalent vegetation and rangeland cover, affecting species types, composition and distribution, as well as those depending on them (Wingqvist and Dahlberg, 2008).

### **3.2 Methods of Data Collection and Processing**

The main aim of data collection was to gather any available information concerning the impacts of ISPAAD on the environment which was the basis for further analysis. In this study, GIS and RS were used to produce LULC maps from 2006 and 2020 Landsat imagery for assessing the severity of land degradation as well as mapping of soil erosion hazards using SLEMSA model in the study area. Methods of data collection and processing were considered separately for each specific objective.

#### **3.2.1 Land use land cover (LULC) determination**

Landsat 5 and 8 satellite images of 3<sup>rd</sup> July 2006 and 10<sup>th</sup> August 2020 were obtained for the purpose of land cover classification. Results of classification were used for description and interpretation of temporal and spatial changes in land cover for the area. The images of path 172 and row 077 (Gaborone area) were downloaded from the United States Geological Survey (USGS) Earth Resources Observation Systems (EROS) data centres under the Landsat Archive (URL: <https://eros.usgs.gov/>).

The image of July 2006 was selected as the historical image for change detection against the August 2020 imagery which was selected to closely match the 2006 image based on seasonal similarities. Both image scenes fell within the dry season; these were periods when the land experienced high rates of vegetation loss. Bare land was easily distinguished and there was no confusion between cultivated land and vegetated land during the classification process. The Landsat images were selected based on the identified similarities as well as the availability of cloud-free images.

The Dinogeng map transformed into Universal Transverse Mercator projection in zone 35'S was used to clip satellite imageries. Ground truth data used were in the form of reference points collected using Global Position System (GPS) together with ground truth points randomly created using ArcMap 10.7 software. Google Earth and Google Earth Pro software were used to validate the randomly created ground truth points for image classification and the overall accuracy of the results.

#### **3.2.2 Image Classification Process**

Image classification was done in order to assign different spectral signatures from the LANDSAT datasets to different LULC categories or classes. This was done on the basis of reflectance features of the different LULC types. Different colour composites were used to improve visibility of various objects on the imagery. Infrared colour composite NIR (4),

SWIR (5) and Red (3) were applied in the identification of varied levels of vegetation and in separating different shades of vegetation. Other colour composites such as Short Wave Infra-red (7), Near Infra-red (4) and Red (2) combination which are sensitive to variations in moisture content were applied in identifying bare soils. This was supplemented by field visits together with the use of high resolution images from Google Earth and Google Earth Pro that made it possible to establish the main land use land cover types. For each of the predetermined LULC type, training samples were selected by delineating polygons around representative sites. Spectral signatures for the respective LULC types derived from the satellite imagery were recorded by using the pixels enclosed by these polygons.

The Geomatica focus tools were used to carry out supervised classification (PCI Geomatics., 2018). Training sites were created using recognizable regions of the satellite image. The training samples were then used to program the computer system to identify pixels with similar characteristics. Training site analysis was then performed to ensure correspondence between spectral classes and information classes. Running of the supervised classification was completed using the maximum likelihood classifier algorithm. The Maximum Likelihood Classification (MLC) algorithm was used as it is the most widely used and accurate of the parametric classifiers. It is based on the probability that a pixel belongs to a particular class. The basic equation assumes that these probabilities are equal for all classes, and that the input bands have normal distributions (Campbell and Wynne, 2011).

In addition, ground truth data were used as a vital reference for supervised classification, accuracy assessment and validation of the result. Furthermore, post classification filtering procedures were done to improve the overall appearance of the map. In this study, post classification of image data was used to remove any unwanted noise and therefore resulting in removal of stray pixels in the image and formation of more homogeneous classes.

### **3.2.3 Accuracy Assessment**

Accuracy assessment procedure was performed on the classified images to determine the success of the process. Accuracy assessment was performed using the standard method of Congalton (1991) which involves firstly, the processes of assessment, identification of references from the ground and the identified references are independent of the ground truths that are used in the classification scheme (Agidew and Singh, 2017). Accuracy assessment process is well documented in literature (Anand, 2018; Bharatkar and Patel, 2013; Campbell and Wynne, 2011; Manandhar et al., 2009; Parece et al., 2011). The classified image of 2006

was compared with image of the same location in Google Earth while the 2020 imagery was compared against image in Google Earth Pro. Using ArcGIS, 240 sets of stratified random points were generated within Dinogeng for each image. Congalton and Green (2009) and Congalton (1991) recommended a minimum of 50 sample points per category. Using the image which is assumed to be correct, the randomly created points were compared on a point-by-point basis to identify each point known in the classified image. The process was completed by compiling an error matrix table which was used for calculation of Overall accuracy, User's accuracy, Producer's accuracy, Errors of Commission & Omission and the Cohen's Kappa coefficient.

Overall Accuracy specifies the correctness of the whole classification and it was calculated by dividing the total number of the correctly classified points (addition of diagonals) to the total number of points (grand total of reference points). The ratio between the number of correctly classified points and the classified totals points of LULC class is the user's accuracy because users are concerned about what percentage of the classes has been correctly classified. The ratio between the number of correctly classified points and the reference total points for LULC class is the producer's accuracy. A more appropriate way of presenting the individual classification accuracies are as follows (Bharatkar and Patel, 2013): Commission error = 1 - user's accuracy or 100 - user's accuracy, while Omission error = 1 - producer's accuracy or 100 - producer's accuracy. The Kappa coefficient ( $K$ ) was computed as follows:

$$K = \frac{P_o - P_c}{1 - P_c}$$

Where,  $P_o$  = proportion of units which agree, = overall accuracy

$P_c$  = proportion of units for expected chance agreement

A Kappa coefficient of 90% may be interpreted as 90% better classification than would be expected by random assignment of classes (Bharatkar and Patel, 2013). Interpretation of Kappa statistics is shown in Appendix 1, so a Kappa value of 90 % falls in the highly ranked statistic number (S. No) 6 rated as almost perfect (Rwanga and Ndambuki, 2017).

### 3.3 Assessment of Soil Fertility

One of the objectives of the study was to assess the impacts of ISPAAD based on soil properties. The chemical properties of the soils for eighteen farmers in Dinogeng were

obtained to assess soil fertility based on availability of information. A comparison was done with the data obtained from national soil map of scale 1: 250 000. The dominant soils in the study area are luvisols.

Soil test results of arable farmers' ploughing fields for the period after inception of ISPAAD (2009 to 2020) were obtained from the Department of Agricultural Research Soil Analytical Laboratory, Agricultural extension officers and the Agricultural District Headquarters at Mochudi. The following soil chemical properties were considered for assessment of soil fertility based on availability of information: soil pH, Organic carbon (OC) and Cation Exchange Capacity (CEC). The analytical soil test report comprised of pH, Organic Carbon (OC), Phosphorus (P), Calcium (Ca), Magnesium (Mg), Potassium (K), and Sodium (Na). Cation exchange capacity was also available in the results between 2009 and 2014. The CEC results for 2015 – 2020 were determined through summation of the cations. Geographical coordinates of the ploughing fields were taken during field work using a GPS.

Baseline data for the selected farmers' ploughing fields was extracted from national soil map of scale 1: 250 000 for comparison purposes. The average CEC and pH data was obtained from the soil map made available by the Soil Mapping Section of the Ministry of Agriculture. Interpretation of the information was done with the use of the Revised General Soil Legend of Botswana (Rommelzwaal and Verbeek, 1990) and Harmonized World Soil Database (FAO et al., 2009). The OC information was gathered from Soil Mapping and Advisory Service Project of the FAO/UNDP (Joshua, 1991). The OC information was then used to estimate soil organic matter (SOM) content using the equation  $SOM (\%) = OC (\%) \times 1.72$  (Hoyle, 2013). The soil test results were then compared to the baseline data.

### **3.4 Mapping of Soil Erosion Hazards**

The SLEMSA input data included rainfall, soil units, slopes and land cover.

#### **3.4.1 Rainfall Energy (E)**

The monthly rainfall amounts of Dinogeng were collected for over 19 years from the Department of Meteorological Services (DMS). Monthly rainfall records from three nearby meteorological stations covering various periods between 1995 and 2019 were used to calculate the mean annual rainfall. Rainfall energy was then determined according to Equation (1) developed by Elwell (1978) for erosive rainfall (Stocking et al., 1988; Vargas and Omuto, 2016). The mean annual rainfall was first interpolated to generate continuous rainfall data for each grid cell by using Analyst Tools Raster Inverse Distance Weighting

(IDW) Interpolation in ArcGIS to create a raster map for the area shown in Fig. 3.2. The rainfall stations were selected based on the availability of complete data and their proximity to the study area. Details of the rainfall stations are presented in Table 3.1.

$$E = 18.846 * \text{MAP} \quad \text{Equation (1)}$$

Where, E is the rainfall energy and MAP is the mean annual precipitation (mm).

**Table 3.1. Meteorological variable records for the stations.**

Station no.	Station ID	Station name	Latitude °S	Longitude °E	Elevation amsl (m)	Annual rainfall mm	Period
1	136	Mochudi Police	24° 23'	26° 8'	945	405	2000 to 2019
2	177	Olifantsdrift Police	24° 12'	26° 41'	855	326	1995 to 2019
3	228	Sikwane Police	24° 25'	26° 27'	915	373	1995 to 2019

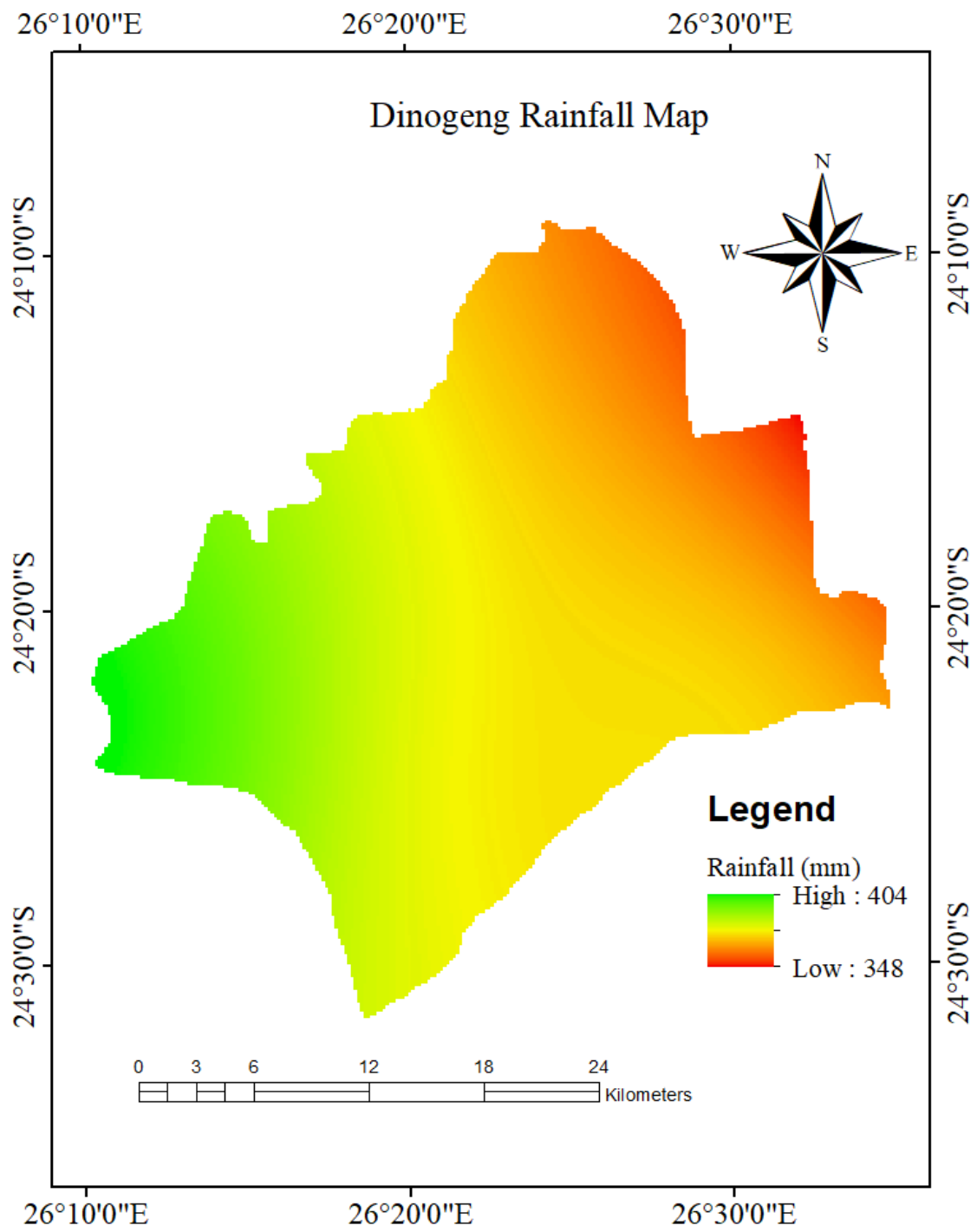


**Fig.3. 2** Dinogeng spatial rainfall variability

### 3.4.2 Soil Erodibility Factor (F)

The soil units' map for the area of interest was extracted from Kgatleng District digital soil map at 1: 250 000 scale by masking using Spatial Analyst Tools within ArcGIS environment. The soil erodibility (F) factor was estimated based on local condition and soil texture (Table 3.2) (Bobe, 2004; Heydarnejad et al., 2020; Tiruneh and Ayalew, 2015; Vargas and Omuto, 2016; Wischmeier and Smith, 1978). The F value increased with declining probability of soil erodibility. The resulting shape file was converted to raster format with a cell size of 30 m x 30 m. The raster map was then reclassified based on their erodibility values.

**Table 3.2. Method of assessing F value (Heydarnejad et al., 2020)**

Soil texture	Soil type	F value
Light	Sands, Loamy sands, Sandy Loams	4
Medium	Sandy clay Loam, Sandy clay	5
Heavy	Clay, Heavy clay	6

### 3.4.3 Slope Length and Slope Steepness

The Shuttle Radar Topography Mission (SRTM) Digital Elevation Model (DEM) of spatial resolution of 30 m (readily available in the Department of Agricultural & Biosystems Engineering) was used to generate slope using Spatial Analyst Tools within ArcMap 10.7 environment. Flow accumulation and slope steepness were then calculated using filled DEM with a Raster Calculator in ArcGIS (Tiruneh and Ayalew, 2015), using Equations (2) and (3).

$$l = \text{Flow accumulation} * \text{cell size} \quad \text{Equation (2)}$$

$$S = (0.43 + 0.30 s + 0.043 s^2)/6.613 \quad \text{Equation (3)}$$

Where  $l$  is the slope length,  $S$  is the slope gradient factor and  $s$  is the gradient (%).

### 3.4.4 Topographic Factor (X)

The Topographic ratio is a product of two factors: a slope gradient factor and a slope length factor. The slope length and slope gradient factors were calculated using the filled DEM and entered into the Equation (4) (Morgan and Davidson, 1991) to produce the topographic factor grid map. To calculate the slope length, derivation of Flow accumulation was based on the DEM after conducting the Fill and Flow direction process respectively in ArcGIS (Bvindi, 2019).

$$X = \sqrt{(l/22.1) (0.065 + 0.045S + 0.0065S^2)} \quad \text{Equation (4)}$$

Where  $X$  is the topographic ratio,  $l$  is the slope length (m) and  $S$  is slope (%).

### 3.4.5 Crop Ratio (C)

The land cover classification generated from Landsat 8 imagery for the year 2020 was used to determine the C-factor. Due to the lack of detailed information and difficulties in processing, C-factor values were assigned to every class in a GIS using a raster calculator, based on literature data in Table 3.3.

**Table 3.3. C-factor values for the study area**

No	Land cover classes	C-factor values	Source
1	Shrub	0.014	Wischmeier, and Smith., 1978
2	Forest	0.01	Hurni., 2016
3	Cultivated land	0.15	Tiruneh and Ayalew., 2015
4	Bare land	0.6	Hurni., 2016, Bvindi, 2019

### 3.4.6 Principal Factor (K)

The value of the K factor was determined by relating mean annual soil loss to mean annual rainfall energy ( $E$ ) using Equation (5) (Morgan, 1995)

$$\ln K = b \ln E + a \quad \text{Equation (5)}$$

Where  $E$  is in  $\text{Jm}^{-2}\text{mm}^{-1}$ ;  $a$  and  $b$  are functions of the soil erodibility factor ( $F$ ):

$$a = 2.884 - 8.2109F \quad \text{Equation (6)}$$

$$b = 0.4681 + 0.7663F \quad \text{Equation (7)}$$

Equations (6) and (7) were substituted into equation (5) to get the final Equation (8) used for estimation of the K factor.

$$K = \exp [(0.4681 + 0.7663*(F)) \ln E + 2.884 + (8.1209*F)] \quad \text{Equation (8)}$$

K factor values were assigned to respective soil types in soil map to generate the soil erodibility map using GIS.

## 3.5 Soil Loss Analysis

The overall procedure involved the use of the SLEMSA model in a GIS environment. The input parameters obtained from meteorological stations, soil map, topographic map, satellite

images and DEM were processed as shown in Fig. 3.3. A cell-by-cell analysis of the soil loss was done to determine annual soil loss rate by overlaying and multiplying the respective SLEMSA sub-model values ( $K$ ,  $C$ , and  $X$ ) interactively by using Spatial Analyst Tool Map Algebra Raster Calculator in ArcGIS 10.7 environment as shown Equation (9).

$$Z = KCX \quad (\text{Elwell, 1978}) \quad \text{Equation (9)}$$

Where,  $Z$  is the predicted mean annual soil loss in  $\text{t}\cdot\text{ha}^{-1}\cdot\text{yr}^{-1}$ ;

$K$  is the mean annual soil loss in  $\text{t}\cdot\text{ha}^{-1}\cdot\text{yr}^{-1}$  from a standard field plot  $30 \times 10$  m with a slope of 4.5% and for a soil of a known erodibility rating  $F$  under a weed-free bare fallow;

$C$  is the ratio of soil lost from a cropped plot to that lost from bare fallow;

$X$  is the ratio of soil lost from a plot of 30 m length  $L$  and slope percent  $S$ , to that lost from the standard plot with a 30 m length and 4.5% slope.

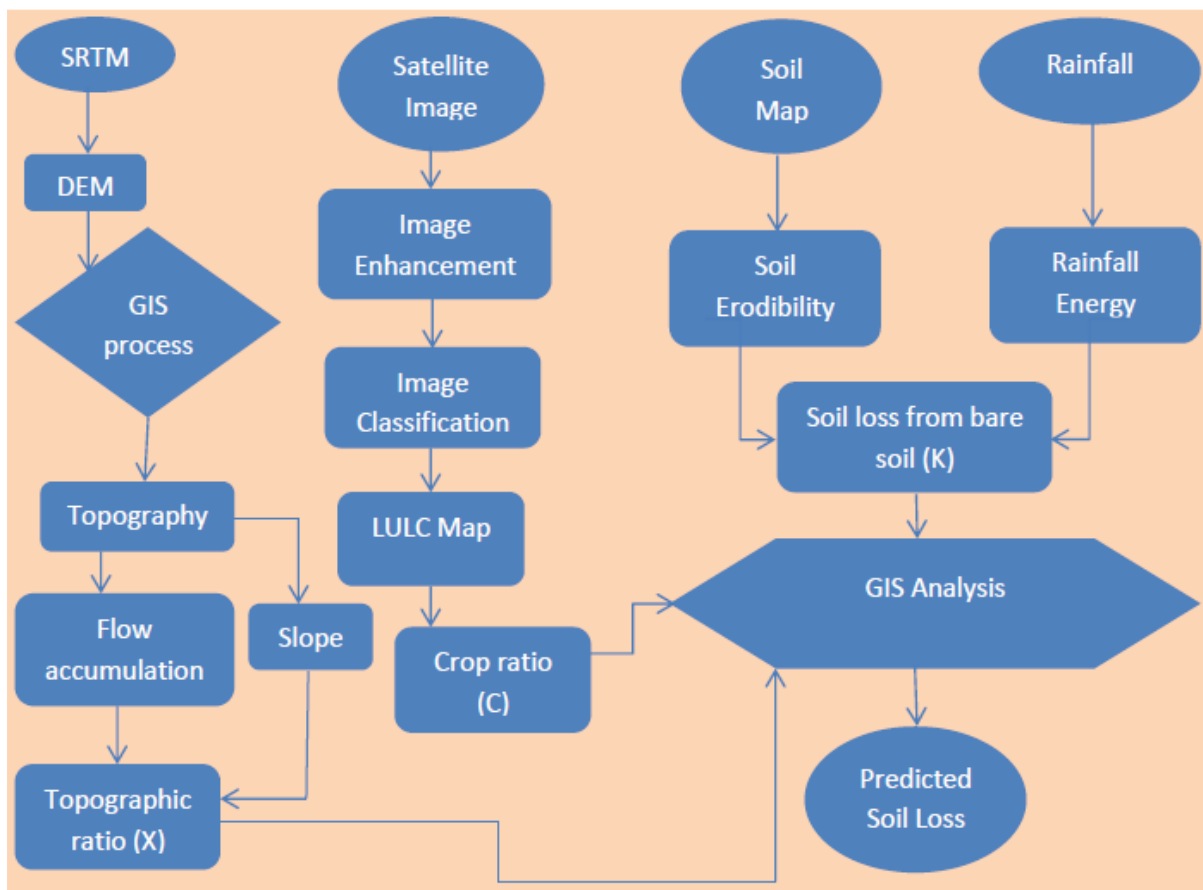


**Fig.3. 3 Flowchart for implementation of SLEMSA model**

The soil loss potential was then categorized into different severity classes according to Marondedze & Schütt (2020) classification to determine erosion risk priority areas for conservation planning.

### 3.6 Software Packages and Data Processing

Geomatica 2018 Catalyst Professional software was used for image processing, and digital image classification or spectral class recognition was accomplished by supervised classification. The classification results (i.e. land cover raster image) were exported into ArcMap 10.7 for accuracy assessment with the aid of high-resolution imagery software, Google Earth and Google Earth Pro. Layers were spatially organised with the same resolution and coordinate system within ArcGIS environment (Parece, et. al., 2011). Microsoft Office was used for presentation, documentation and pre-processing calculations in excel environment. The GeoConverter-Geoplaner software package was used for converting geographical coordinates. Table 3.4 presents a summary of the software packages and their applications.

**Table 3.4. Software packages and their applications**

<b>Software package</b>	<b>Application</b>
<b>Geomatica (Catalyst Professional)</b>	Satellite image pre-processing and Land cover classification
<b>ArcMap 10.7</b>	Database creation, Dataset preparation, Raster calculation and Accuracy assessment
<b>Microsoft Office</b>	Presentation, Documentation and Calculation
<b>Google Earth and Google Earth Pro</b>	Aids in validation of ground truthing process for accuracy assessment
<b>Geo-Converter</b>	Conversion of coordinates

## CHAPTER 4: RESULTS AND DISCUSSION

### 4.1 Land use land cover change (LULCC) detection

Data interpretation and analysis for the study area is based on the comparison of LULC changes for the 14-year (2006-2020) period.

#### 4.1.1 Image Classification

Table 4.1 describes the land cover classes used for the classification process. Spatial distribution of LULC for the given period is shown in Fig. 4.1. The 2006 satellite image was classified into four classes, with 19.7% (16382 ha) of the area covered with cultivated land, 11.5% (9530 ha) with bare land, 7.2% (6011 ha) with forest and 61.6% (51194 ha) with shrubs. About 39% (32478 ha) of the area of the 2020 image is classified as cultivated land, 29.7% (24711 ha) as bare, 6.5% (5434 ha) as forest, and 24.7% (20495 ha) as shrub land.

**Table 4.1. LULC class description for the classification process**

No	LULC class	LULC class description
1	Cultivated land	The land which is mainly used for growing food crops such as maize, sorghum, millet, beans, cowpeas, lablab, and other fodder crops. Crops in this land are rain-fed. Fallow land is also lumped here.
2	Bare land	This describes the land left without vegetation cover. This results from abandoned crop land, eroded land due to land degradation, gravel road surface and dry pan.
3	Forest land	This describes the areas with evergreen trees mainly growing naturally in the reserved land, along the rivers and on the hills.
4	Shrub land	Areas with natural pastures, scrub grass, sparse trees and shrubs.

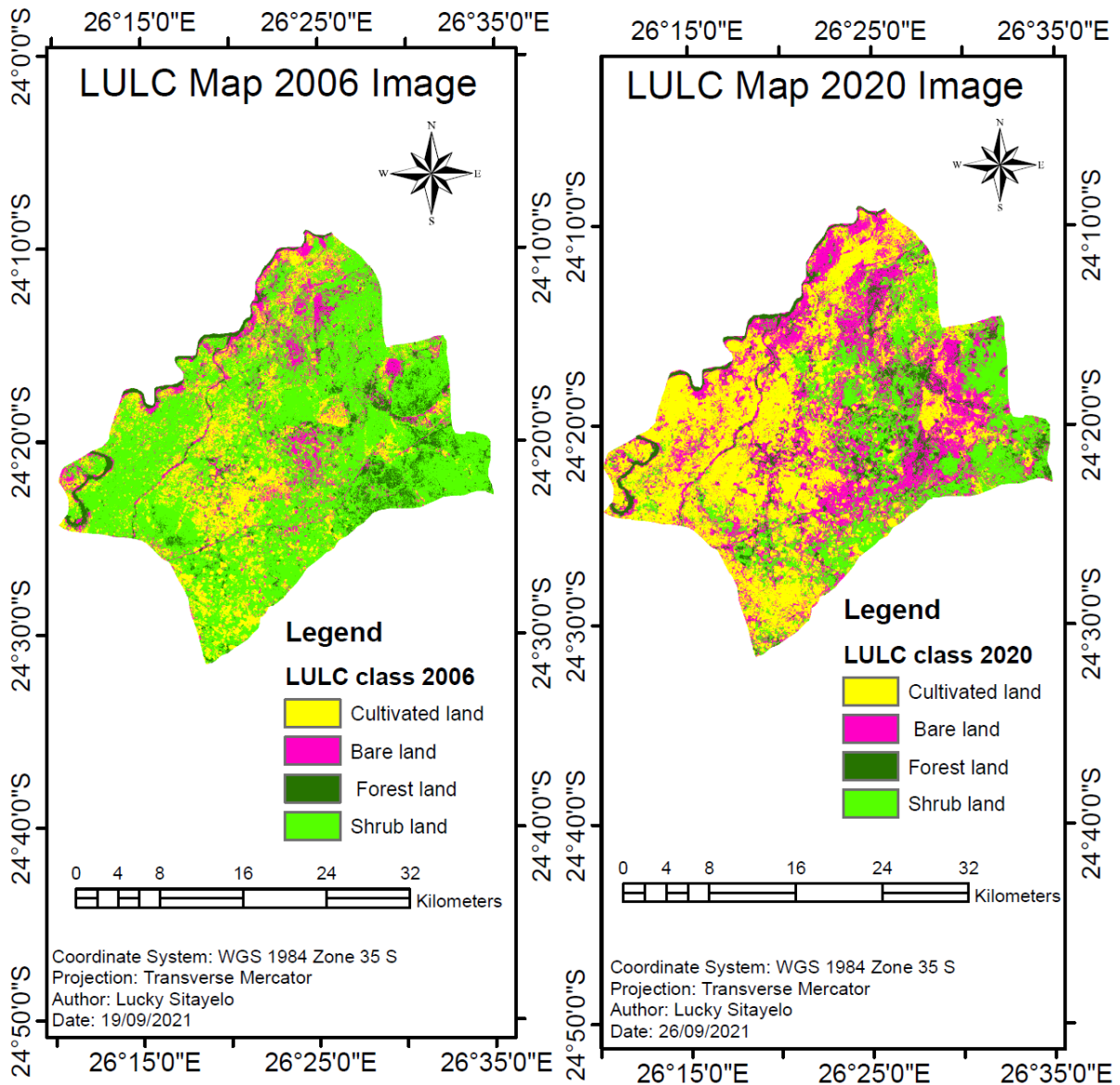


**Fig.4. 1 LULC classification maps (2006 and 2020)**

#### 4.1.2 LULC change detection

The results obtained after processing the two multispectral datasets of Landsat 5 and 8 for LULC change detection are given in Table 4.2. Bare land and cultivated land increased by 18.3 and 19.4%, whereas forest areas and shrub land declined by 0.7 and 36.9%, respectively, over the period.

#### 4.1.3 LULC Change Analysis

The result of this study showed that cultivated and bare areas increased by 16,096 and 15,181 hectares, respectively. Evergreen forests decreased by 577 ha whereas shrub land declined by 30,699 ha over the same period. The results are shown in Table 4.2 and appendix 3; Bar chart depicting LULCC in percentage. These changes took place at the expense of other LULC classes. These LULC changes are complex and at the same time interrelated such that the

expansion of one LULC type occurs at the expense of other LULC classes (Cheruto et. al, 2016).The results of this study agree with those of other studies.

**Table 4.2.The LULC change detection for 2006 and 2020 of Dinogeng**

No	classes	2006		2020		2020 - 2006
		Area (ha)	Area %	Area (ha)	Area %	% Difference
1	Cultivated land	16382	19.7	32478	39.1	+ 19.4
2	Bare land	9530	11.5	24711	29.7	+ 18.2
3	Forest	6011	7.2	5434	6.5	- 0.7
4	Shrubs	51194	61.6	20495	24.7	- 36.9
<b>Total</b>		83117	100.0	83117	100.0	0.0

A study by Gete and Hurni (2001) found that the expansion of cultivated land took place at the expense of forest land between 1957 and 1982 in the North-western Ethiopian highlands. Similarly, recent researches have revealed that the expansion of agricultural land has been at the expense of lands with natural vegetation cover (Amsalu et al., 2006; Lambin and Geist, 2001; Schneider and Pontius, 2001).

Expansion of cultivated land is related to the introduction of the ISPAAD subsidy programme by government together with increase in population. The BCA Consult (2012) reported that, Botswana had a total of 31, 000 arable farmers before ISPAAD started in 2007/08 but the number of ISPAAD beneficiaries increased to 96,000 in 2008/09 until it reached 118,000 in 2010/11. Furthermore, the area of land planted was 104,000 ha in 2007/08. This area increased to 298,000 ha in 2008/09 until it reached 377,000 ha in 2010/11.

The population of Kgatleng district increased from 73, 507 to 91,660 in the period between 2001 and 2011 (Statistics Botswana, 2014). Kgatleng has an area of 7, 960 km<sup>2</sup> and the population density of the district increased from 9.2 to 11.5 persons per km<sup>2</sup> in the reported period. The annual population growth rate for Kgatleng recorded between 2001 and 2011 was 2.2 percent. Due to population increase as well as positive response by farmers towards the ISPAAD programme, there was high demand for land for cultivation resulting in deforestation. The area which was initially covered by vegetation was converted into arable and bare land. Bare areas increased by 15,181 ha resulting in a sharp rise of 18.2 %. This statistic implies that, on average, about 1.3% of the total area of Dinogeng is exposed to

vagaries of rainfall annually. Agriculture has been reported to be the main reason behind such land use changes resulting in soil erosion (Tesfamichael, 2004). It starts with removal of the natural vegetation cover thereby exposing the soil to any kind of external actions that lead to its removal. Cultivation causes disturbance of the topsoil layer and since crops are seasonal or short-lived, they are removed after the harvest, thus leaving the soil vulnerable to dislocation. A study on the effect of cultivation on soil loss by Choudhary et al. (1997) reported that soil erosion and runoff were highest for mouldboard-ploughed areas and least for no-till soil.

In addition to cultivation, overgrazing is also an important cause of vegetation clearance and subsequent soil erosion. The LULC classification results show that the rate of deforestation is approximately 2.7% per year or 2, 234 ha of vegetated land are lost annually. Removal of the topsoil negatively impacts on the agricultural productive capacity of the land resource. Uncontrolled or poorly managed grazing brings about removal of vegetation that exposes the soil to all types and processes of erosion. Land degradation has been reported to be a serious environmental problem (Wingqvist and Dahlberg, 2008), especially in the eastern parts of Botswana due to the growing human population with increased number of livestock resulting in overgrazing as well as the use of inappropriate farming techniques. Kgatleng District is relatively small and under immense pressure from different land uses (Tshireletso et al., 2018). Like most communal parts of Botswana, the area of study is open to both arable farming and open-access communal livestock grazing which is characterized by smallholder farmers who are also lacking in management of the land resources. Multiple land use involving high stocking densities of different livestock species, destruction of tree species for domestic purposes (fire wood, construction of livestock fencing and field fencing) and land clearing for arable farming was associated with the significantly low tree species density in the Mmamolongwana communal area (Mugabe et al., 2017).

#### **4.1.4 Accuracy Assessment**

In this study, accuracy assessment was performed for the classified maps of all the two time steps: 2006 and 2020. Stratified random sampling design was adopted for the accuracy assessment. All the four LULC classes were considered for accuracy assessment. The error matrix shown in Tables 4.3 and 4.4 was used for calculation of User's accuracy, Producer's accuracy, Errors of Commission & Omission and the Cohen's Kappa coefficient to determine the success of the classification process.

For 2006 LULC, the map results were: overall accuracy of 93%, User's accuracy of 90 - 100% and producer's accuracy of 75 - 100 %. The overall accuracy for 2020 LULC map was better with 94% whilst the other two accuracies had 88 - 100%. Producer's accuracy is defined as the probability that any pixel in that category has been correctly classified (Anand, 2018). The cultivated category of Table 4.3 for, has accuracy of 75% meaning that approximately 75% of the cultivated ground truth pixels also appear as cultivated pixels in the classified image. User's accuracy is the probability that a pixel classified on the image actually represents that category on the ground. The cultivated category of Table 4.3 for example, has reliability of 100% meaning that all the cultivated pixels in the classified image actually represent cultivated land on the ground. From Producer's accuracy and User's accuracy values for different classes given in Table 4.3 and 4.4, it can be concluded that the test set classes bare and shrub were difficult to classify: a good number of pixels were excluded from those categories, thus the areas of these classes in the classified image are probably underestimated. On the other hand, cultivated land in the image is not very reliable as some pixels of other categories were included in the cultivated land category in the classified image. Thus, the area of cultivated land category in the classified image is probably overestimated.

The diagonal elements in the matrices represent the number of correctly classified points of each class. In the error matrix of 2006 image (Table 4.3), for example, 132 pixels/points of shrub land in the test set were correctly classified as shrub in the classified image. On the other hand, off-diagonal elements represent misclassified pixels or the classification errors, i.e. the number of ground truth points that ended up in another class during classification. Fifteen points of shrub in the test set were classified as cultivated in the classified image. The off-diagonal row elements represent ground truth points of a certain class which were excluded from that class during classification (viz. error of omission). For example, 1 ground truth pixel of bare land was excluded from the bare class in the classification and ended up in the cultivated land class (Table 4.3). Off-diagonal column elements represent ground truth pixels of other classes that were included in a certain classification class (viz. error of commission). For example, 15 ground truth pixels of shrub land (in Table 4.3) were included in the cultivated land class by the classification.

In this study an overall Kappa coefficient of 0.89 was obtained for the 2006 LULC map and 0.92 for 2020 LULC map. Kappa coefficient expresses a proportional reduction in error produced by the classification process, compared with the error of a completely random

classification. According to Lillesand et. al (2015) kappa statistic serves as an indicator of the extent to which the percentage correct values of an error matrix are due to “true” agreement versus “chance” agreement. As true agreement (observed) approaches 1 and chance agreement approaches 0, kappa approaches 1. For example: a value of 0.89 implies that the classification process was avoiding 89% of the errors that a completely random classification would generate. Kappa coefficients of 0.89 and 0.92 may be interpreted as 89% and 92% better classification than would be expected by random assignment of classes. Kappa statistic ranging between 80% - 100% is rated as almost perfect (Rwanga and Ndambuki, 2017) and greater than 75% excellent (Bharatkar and Patel, 2013). The summary for the error matrices for 2006 and 2020 is shown in Appendix 2.

**Table 4.3. Error matrix for 2006 classified map**

	<b>Cultivated</b>	<b>Bare</b>	<b>Forest</b>	<b>Shrub</b>	<b>Totals</b>	<b>UA</b>	<b>CE</b>	<b>Kappa</b>
	<b>land</b>							
<b>Cultivated</b>	<b>47</b>	0	0	0	47	100%	0%	
<b>Bare land</b>	1	<b>27</b>	0	0	28	96%	4%	
<b>Forest</b>	0	0	<b>18</b>	0	18	100%	0%	
<b>Shrub</b>	15	0	0	<b>132</b>	147	90%	10%	
<b>Totals</b>	63	27	18	132	<b>240</b>			
<b>PA</b>	75%	100%	100%	100%		<b>93%</b>		
<b>OE</b>	25%	0%	0%	0%				
<b>Kappa</b>								<b>0.89</b>

**PA:(Producer’s accuracy), UA:(User’s accuracy), OE: (Omission error),**

**CE:(Commission error)**

**Table 4.4. Error matrix for 2020 classified map**

LULC	Cultivated	Bare land	Forest	Shrub	Totals	UA	CE	Kappa
<b>Cultivated</b>	94	0	0	0	94	100 %	0 %	
<b>Bare land</b>	6	64	1	0	71	90 %	8 %	
<b>Forest</b>	0	0	16	0	16	100 %	0 %	
<b>Shrub</b>	7	0	0	52	59	88 %	12 %	
<b>Totals</b>	107	64	17	52	240			
<b>PA</b>	88 %	100 %	94 %	100 %		94 %		
<b>OE</b>	12 %	0 %	6 %	0 %				
<b>Kappa</b>								0.92

## 4.2 Assessment of Soil Fertility

### 4.2.1 Baseline Data

Figure 4.2 shows locations of the ploughing fields in the study area. Figure 4.3 shows the topographical input features of the study area whereas primary soil characteristics are given in Table 4.5.

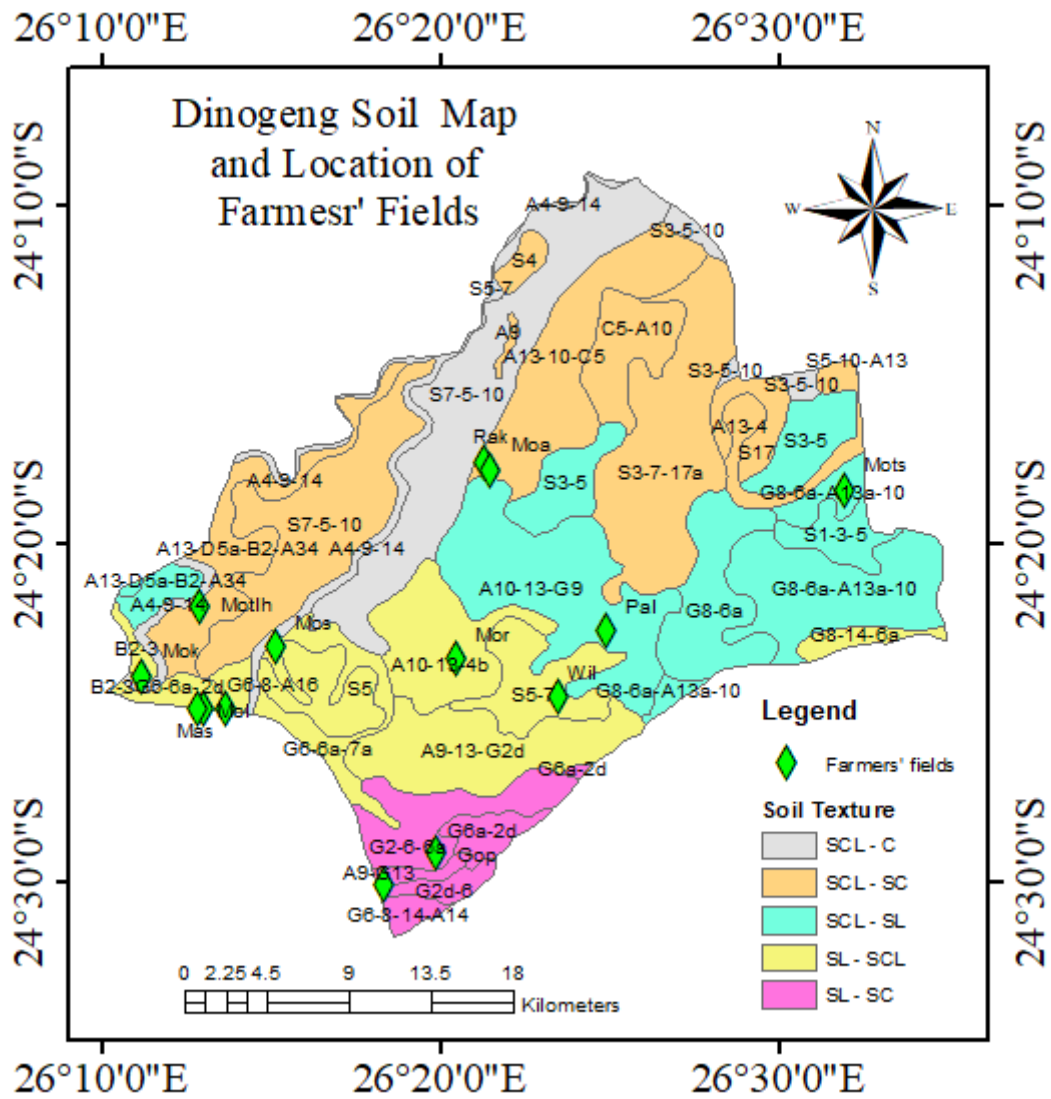
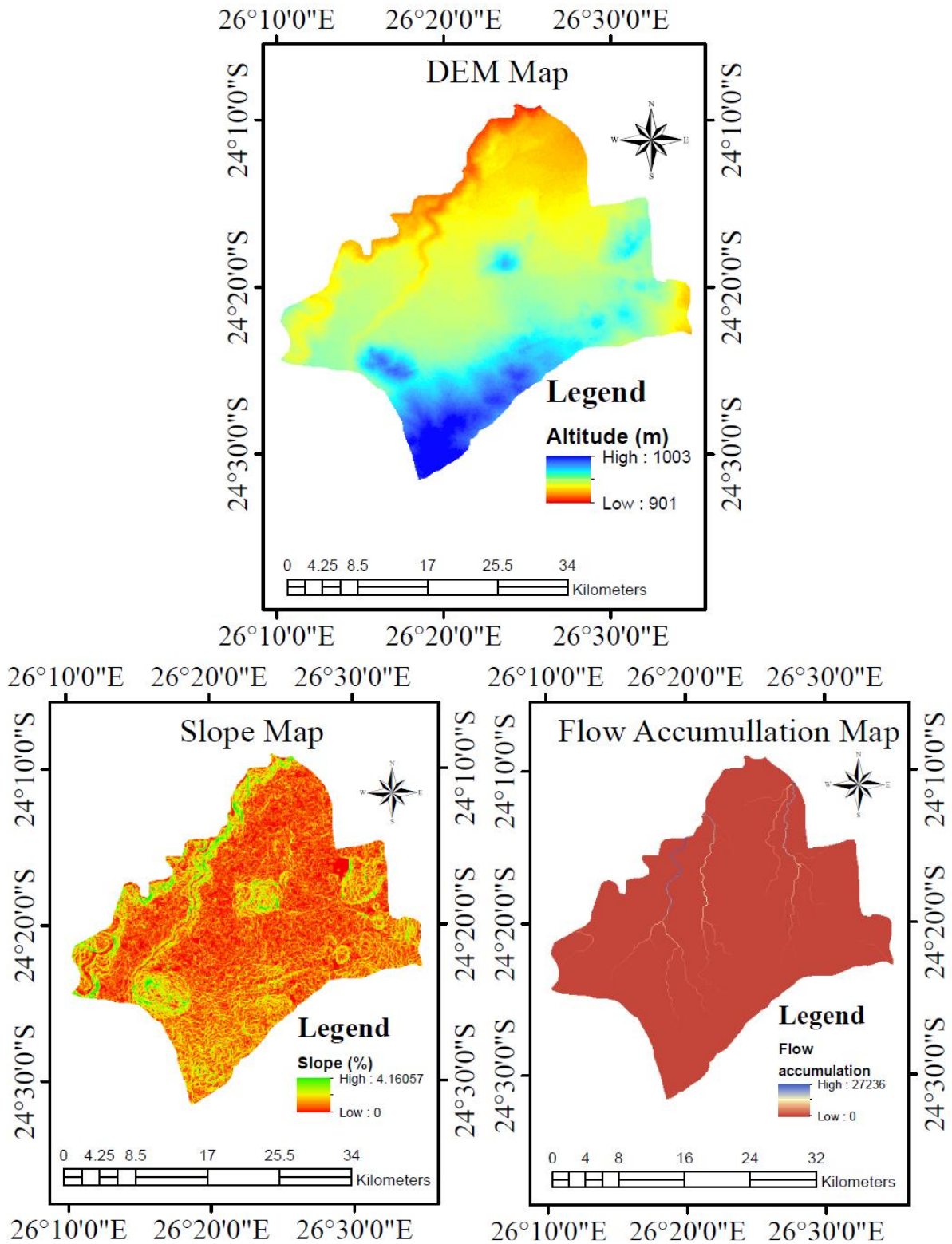


Fig.4. 2 Location of farmer's fields and soils of Dinogeng



**Fig.4. 3 Topographic Ratio input factors and DEM**

**Table 4.5. Soil characteristics of the study area**

<b>No</b>	<b>Field code</b>	<b>Soil unit codes</b>	<b>Unit description FAO (1988)</b>	<b>Texture</b>	<b>pH</b>	<b>OC (%)</b>	<b>CEC (Cmol/kg)</b>
1	Mok	B2-3	Chromic luvisol	SL-CL	5.76	0.66	15.00
2	Mos	G6-6a-7a	ArenicFericluvis ol	LS-SL	6.96	0.33	7.00
3	Mod	G6-8-A16	ArenicFericluvis ol	LS-SL	6.96	0.33	7.00
4	Motl	A13-D5a-B2- A34	Chromic luvisol	SL-SCL	6.96	0.66	7.00
5	Moa	A13-10-C5	Chromic luvisol	SL-SCL	5.01	0.66	15.00
6	Rak	A13-10-C6	Chromic luvisol	SL-SCL	5.01	0.66	15.00
7	Mor	A10-13-4b	Chromic calcic luvisol	SL-SCL	5.01	0.66	15.00
8	Wil	S5-7	FerrallicArenosol	SL-LS	6.96	0.20	2.00
9	Pal	A10-13-G9	Chromic calcic luvisol	SL-SCL	6.96	0.66	7.00
10	Gop	G2-6-6a	ArenicFericluvis ol	LS-SL	6.96	0.33	2.00
11	Moth	A9-G13-G2d-6	Calcic luvisol	SL-C	5.01	0.85	15.00
12	Mol	G6-6a-2d	ArenicFericluvis ol	LS-SL	6.96	0.33	2.00
13	Mas	G6-6a-2d	ArenicFericluvis ol	LS-SL	6.96	0.33	2.00
14	Mph	G6-8a-A16	ArenicFericluvis ol	LS-SL	6.96	0.33	7.00
15	Lot	A4-9-14	CalcaricCambis ol to calcic luvisol	SL-SC	6.96	0.66	15.00
16	Pos	G8-6a-A13-10	Chromic petriccalcic	SCL-C	6.96	0.66	15.00

			luvisols				
<b>17</b>	Phe	A13-10	Chromic calcic	SL-SCL	6.96	0.66	7.00
			luvisol				
<b>18</b>	Mots	G8-6a-A13-10	Chromic petric	SCL-C	6.96	0.66	15.00
			calcic luvisols				

*Soil texture interpretation: S; sands/sandy: L; loam/loamy: C; clay: SL-LS; sandy loam to loamy sands; SCL-C; sandy clay loam to clay*

Source: Soil map of Botswana (1988)

#### 4.2.2 Comparison of Soil Parameters before and after ISPAAD

The overall results before and after ISPAAD generally show a decline in all the three soil parameters (Table 4.6). The pH of the baseline data ranged from 6.96 to 5.01 indicative of neutral to strongly acidic soils. After the inception of ISPAAD, pH ranged from 6.11 to 4.06 indicating slightly acidic to extremely acidic soils. The OC percentage ranged between 0.20 % (low) and 0.85% (sufficient) before ISPAAD, and between 0.02% (very low) and 0.75% (average enough) thereafter. Cation exchange capacity (CEC) values ranged between 2.00–15.00 Cmol/kg before, and between 0.80 – 5.62 Cmol/kg after ISPAAD. Sandy soils generally have a very low CEC of less than 3 Cmol/kg while heavier clay soils have a much higher CEC greater than 20 Cmol/kg (Ketterings et. al, 2007). As Table 4.6 shows, the CEC conspicuously declined in the study area over an 11-year period (2009 - 2020).

**Table 4.6. Soil parameters in the study area before and after ISPAAD**

No	NAME	BEFORE ISPAAD			AFTER ISPAAD		
		pH	OC (%)	CEC(Cmol/kg)	pH	OC (%)	CEC(Cmol/kg)
<b>1</b>	Mokgadi T.	5.76	0.66	15.00	4.37	0.29	3.14
<b>2</b>	Mosate P.	6.96	0.33	7.00	4.93	0.19	2.20
<b>3</b>	Modisagae N.	6.96	0.33	7.00	4.17	0.13	1.77
<b>4</b>	Motlhabane M.	6.96	0.66	7.00	4.78	0.35	4.31
<b>5</b>	Moatshe M.	5.01	0.66	15.00	5.00	0.75	3.30
<b>6</b>	Rakereng T.	5.01	0.66	15.00	6.11	0.39	4.41
<b>7</b>	Moroke R.	5.01	0.66	15.00	4.61	0.29	2.00
<b>8</b>	William D.	6.96	0.20	2.00	4.90	0.20	2.15
<b>9</b>	Palai A.	6.96	0.66	7.00	5.03	0.34	1.83
<b>10</b>	Gopolang E.	6.96	0.33	2.00	5.00	0.75	1.80
<b>11</b>	Mothibe L.	5.01	0.85	15.00	5.00	0.75	1.06
<b>12</b>	Molatlhegi L.	6.96	0.33	2.00	4.06	0.23	1.35
<b>13</b>	Masupu K.	6.96	0.33	2.00	4.93	0.11	3.63
<b>14</b>	Mphusu C.	6.96	0.33	7.00	4.40	0.10	2.07
<b>15</b>	Lotsoalo K.	6.96	0.66	15.00	5.80	0.34	5.62

<b>16</b>	Poswane D.	6.96	0.66	15.00	6.00	0.75	0.80
<b>17</b>	Pheto R	6.96	0.66	7.00	5.00	0.75	4.50
<b>18</b>	Motshabi M.	6.96	0.66	15.00	4.28	0.02	2.56

Soil pH influences the solubility of nutrients. It also affects the activity of micro-organisms responsible for breaking down organic matter and most chemical transformations in the soil. Soil pH thus affects the availability of several plant nutrients. A pH range of 6 to 7 is generally most favourable for plant growth because most plant nutrients are readily available in this range (USDA Natural Resources Conservation Service, 1998). However, some plants have soil pH requirements above or below this range. According to FAO (2015), optimum availability of nutrients occurs around pH = 6.5; toxic concentrations of H and Al occur when the pH drops below 5.5; values of pH above 7.2 indicate an alkaline reaction and may be symptomatic for the immobilization of nutrients.

Soil organic matter (SOM) content is directly influenced by soil texture and moisture content (FAO, 2015). Clay rich soils have higher carbon content compared to sandy soils which are characterised by lower carbon contents. Moist and well-aerated soils are optimal for microbial activity. Decomposition rates consequently decrease as soils become drier. However, flooded soils have lower rates of organic matter decay due to restricted aeration. High precipitation may also lead to carbon transport down the soil profile as dissolved and/or particulate organic matter. During extreme events, such as drought, SOM decomposition may initially decrease but may subsequently increase after rewetting. In this study, the overall decline in OC resulted in the decrease of SOM content during the reporting period. Table 4.7 shows the SOM noticeable general decline over the 11-year period

**Table 4.7. Estimation of SOM content in the study area before and after ISPAAD**

No	NAME	BEFORE ISPAAD		AFTER ISPAAD		SOM Diff (%)
		OC (%)	SOM (%)	OC (%)	SOM (%)	
<b>1</b>	Mokgadi T.	0.66	1.135	0.29	0.499	-0.64
<b>2</b>	Mosate P.	0.33	0.568	0.19	0.327	-0.24
<b>3</b>	Modisagae N.	0.33	0.568	0.13	0.224	-0.34
<b>4</b>	Motlhabane M.	0.66	1.135	0.35	0.602	-0.53
<b>5</b>	Moatshe M.	0.66	1.135	0.75	1.290	0.15
<b>6</b>	Rakereng T.	0.66	1.135	0.39	0.671	-0.46
<b>7</b>	Moroke R.	0.66	1.135	0.29	0.499	-0.64
<b>8</b>	William D.	0.20	0.344	0.20	0.344	0.00

<b>9</b>	Palai A.	0.66	1.135	0.34	0.585	-0.55
<b>10</b>	Gopolang E.	0.33	0.568	0.75	1.290	0.72
<b>11</b>	Mothibe L.	0.85	1.462	0.75	1.290	-0.17
<b>12</b>	Molatlhegi L.	0.33	0.568	0.23	0.396	-0.17
<b>13</b>	Masupu K.	0.33	0.568	0.11	0.189	-0.38
<b>14</b>	Mphusu C.	0.33	0.568	0.1	0.172	-0.40
<b>15</b>	Lotsoalo K.	0.66	1.135	0.34	0.585	-0.55
<b>16</b>	Poswane D.	0.66	1.135	0.75	1.290	0.15
<b>17</b>	Pheto R	0.66	1.135	0.75	1.290	0.15
<b>18</b>	Motshabi M.	0.66	1.135	0.02	0.034	-1.10

Cation exchange capacity and base saturation are important soil measurements that help determine how a soil is managed and fertilized. High CEC indicates high nutrient storage capacity. However, in combination with low pH large amounts of exchangeable aluminium are likely to be present and this has a negative effect on plant growth (Breitbart, 1988). Low CEC also indicates low amounts or absence of primary weatherable minerals and accumulation of secondary clay minerals such as kaolinite due to extensive weathering. High CEC is normally associated with soils having appreciable amounts of weatherable primary minerals as nutrient reserve.

The higher the CEC the more clay or organic matter present in the soil (Ketterings et. al., 2007). This usually means that high CEC (clay) soils have a greater water holding capacity than low CEC (sandy) soils. Low CEC soils are more likely to develop potassium and magnesium (and other cation) deficiencies, while high CEC soils are less susceptible to leaching losses of these cations. So, for sandy soils, a large one-time addition of cations e.g. potassium can lead to large leaching losses. More frequent additions of smaller amounts are better. The lower the CEC, the faster the soil pH will decrease with time. So, sandy soils need to be limed more often than clay soils. The higher the CEC, the larger the quantity of lime that must be added to increase the soil pH; sandy soils need less lime than clay soils to increase the pH to desired levels. There is a positive correlation between CEC and SOM content. Decline in CEC negatively impacts on environmental conditions and crop yields. Thus, the ability of the soil to hold onto and supply nutrients to plants is reduced resulting in low crop and pasture yields. A decline in the resilience of the land to dry periods is very likely due to reduction in microbial activity and water holding capacity. Farmers use poor farming techniques and there is high possibility of increase in fertilizer use in the long-term. The potential to increase fertilizer use in the long-term is associated with lower levels of soil

cover and more soil disturbance and increased erosion risk. Therefore, reduction in CEC (as shown in Table 4.6) has contributed to soil fertility decline and land degradation in the area of study.

### 4.3 Mapping of Soil Erosion Hazards

Mapping of soil erosion hazards in the study area was carried out according to SLEMSA model. The SLEMSA model includes topographic indices derived from the DEM, climatic factors, vegetation or protective role of plants and soil characteristics.

#### 4.3.1 Topographic Ratio (X)

The DEM, slope and flow accumulation maps are presented in Fig 4.3. The input factors were combined to determine the topographic factor map using Equation (4). The topographic ratio ranged from 0 to a maximum of 41.2 as observed in Fig. 4.4. The findings show that the slope and flow accumulation are heavily influenced by altitude and by increasing their values, the topographic ratio factor also implies an increasing trend.

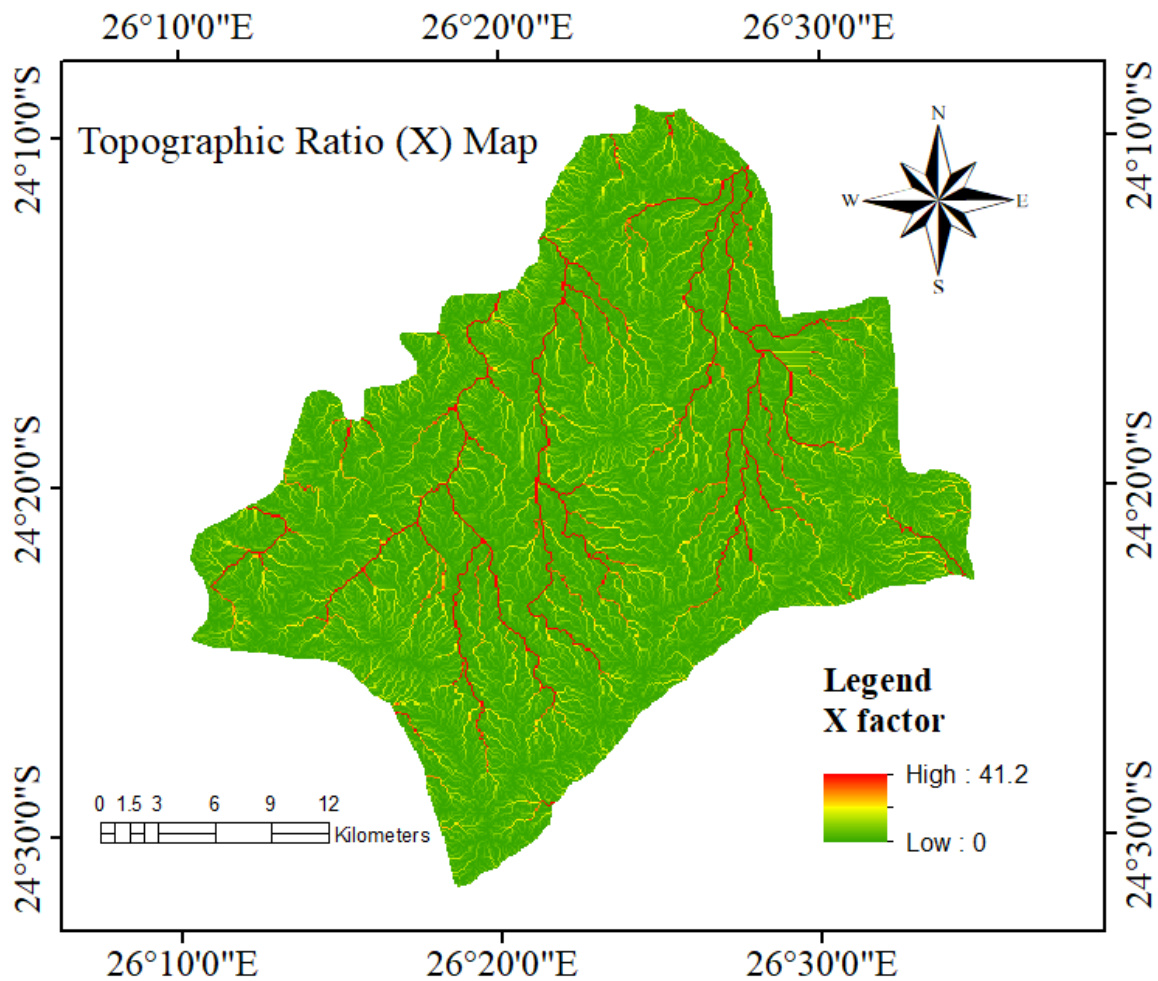


**Fig.4. 4 Topographic ratio (X factor) map**

#### **4.3.2 Rainfall Energy (E)**

Soil loss is closely related to rainfall partly through the detaching power of raindrops striking the soil surface and partly through the contribution of rain to runoff. The mean annual precipitation data interpolated over the entire study area using IDW interpolation technique was converted to rainfall energy by applying Equation (1). The annual rainfall of Dinogeng ranges from 347.8 mm to 403.9 mm (Fig 3.2). The result showed that the average E factor value in the study area was 7071 MJmmha<sup>-1</sup> year<sup>-1</sup> ranging from 6554 MJmmha<sup>-1</sup> to 7612 MJmmha<sup>-1</sup> as shown in Fig 4.5.

#### **4.3.3 Soil Erodibility Factor (F)**

Soil erodibility is regarded as a function of the soil texture, organic matter content, soil structure and the degree of permeability (Maronedze & Schütt, 2020). Soils being highly susceptible to erosion have soil erodibility values close to 1, whereas corresponding values close to 10 indicate a resistive nature of the soil as shown in Fig 4.5. In the current study, information on soil structure and profile permeability was not available. Therefore, the F factor was appraised based on soil texture as shown in Table 3.2.

#### **4.3.4 Principal Factor (K)**

After calculating the values of F and E, the value of K was calculated using Equation 8 in a GIS environment to produce a map. The results show that the K factor ranges between 1.1 tha<sup>-1</sup>yr<sup>-1</sup> to 7.2 tha<sup>-1</sup>yr<sup>-1</sup> (Fig 4.5) with an average value of 2.5 tha<sup>-1</sup>yr<sup>-1</sup>.

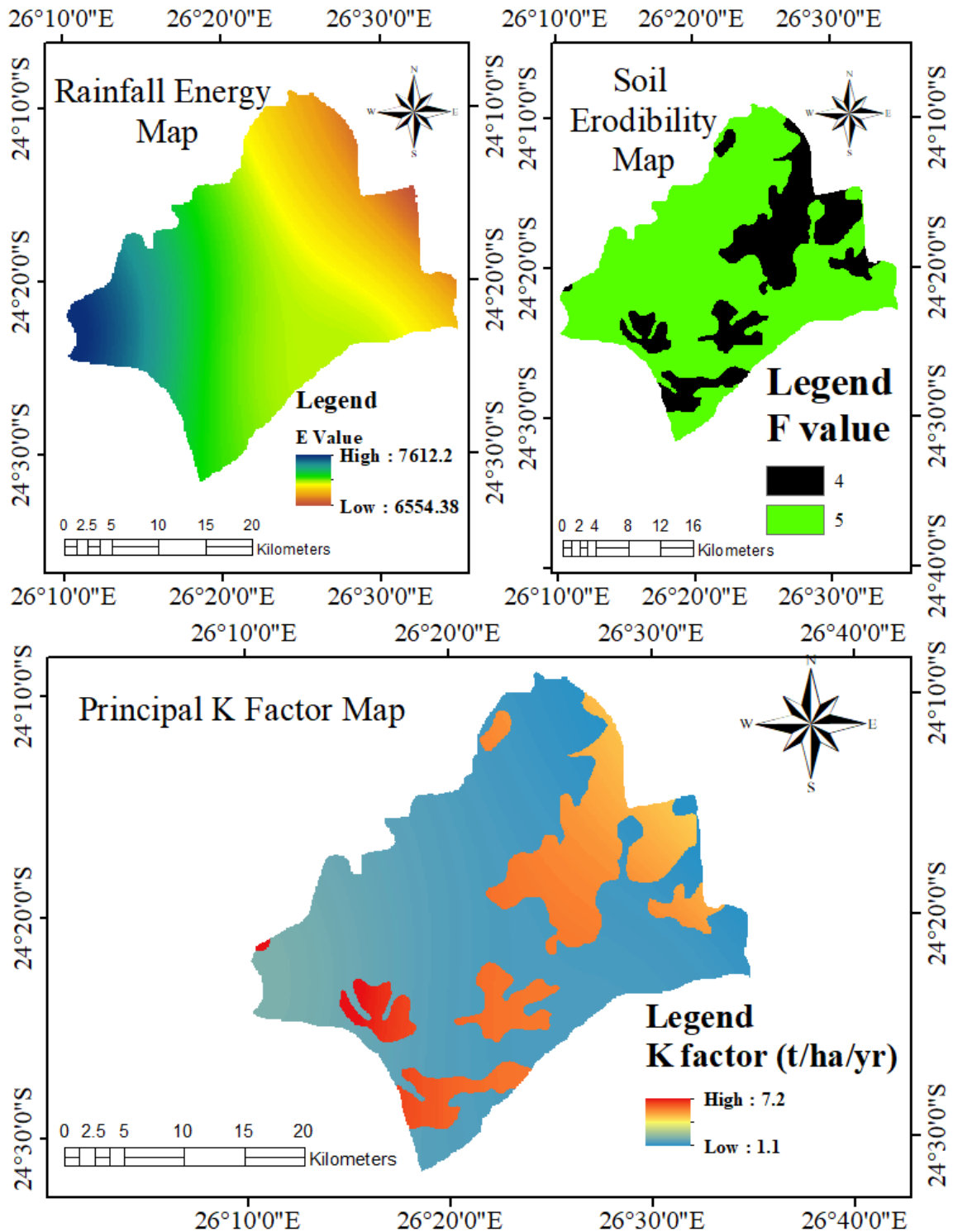


**Fig.4. 5 Principal K and input factors**

#### 4.3.5 Crop Ratio (C) Factor

To evaluate and determine the crop ratio or vegetation factor; indicating the amount of soil loss at bare surfaces and the effect of vegetation on soil conservation, C-factor values were assigned to every LULC class in a GIS using a raster calculator, based on literature data in

Table 3.3 and the values ranged from 0.01 to 0.6 as shown in Fig 4.6. Vegetation factor (C) was estimated based on the type of land-use with bare land being assigned a value of 0.6, cultivated land to 0.15, forest to 0.01 and shrub land to 0.014.

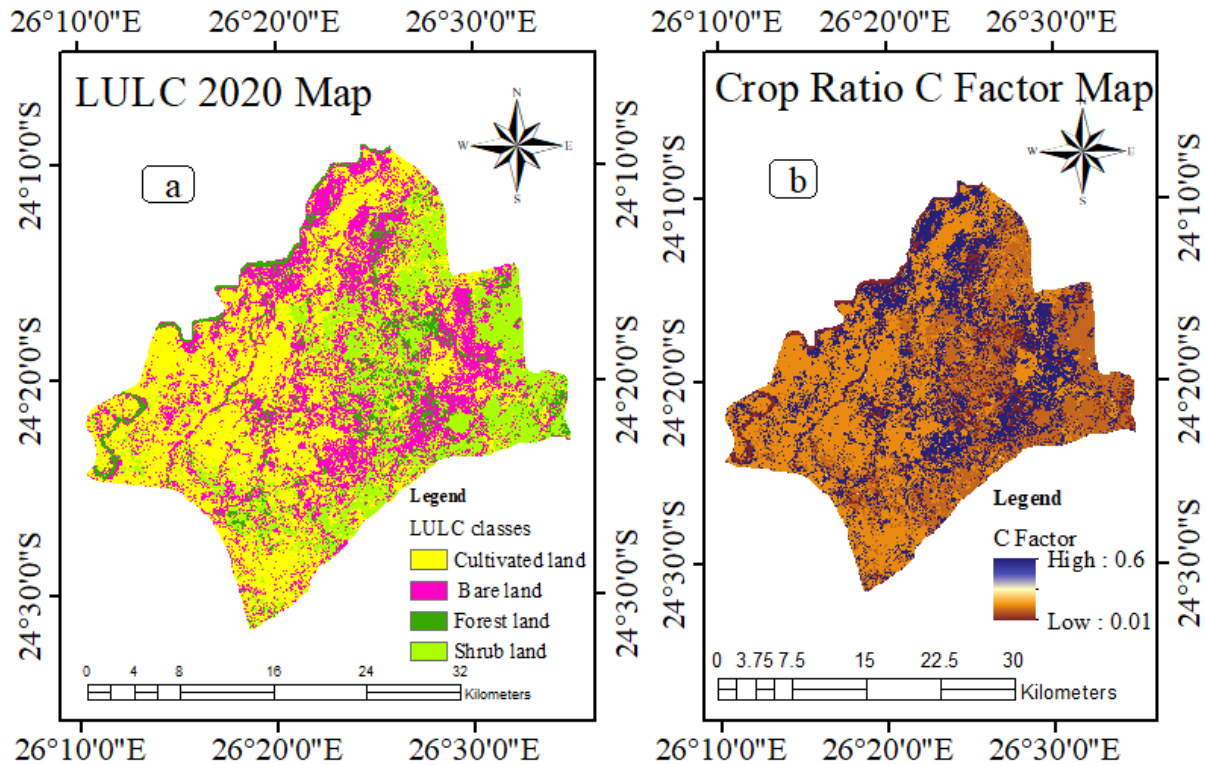


**Fig.4. 6 Spatial distribution of (a) LULC for 2020 and (b) Crop ratio**

#### 4.3.6 Determination of SLEMSA model (Z)

As indicated in section 3.5, the SLEMSA model combines three variables of the topographic factor (X), soil loss due to the soil erodibility (K) and crop ratio factor (C). The calculation of erosion in this model is carried out through equation  $Z = KCX$  (Elwell, 1978) to obtain the annual soil loss map shown in Fig. 4.7. The results were then used to determine different categories of erosion risk areas shown in Table 4.8 and Fig. 4.8.

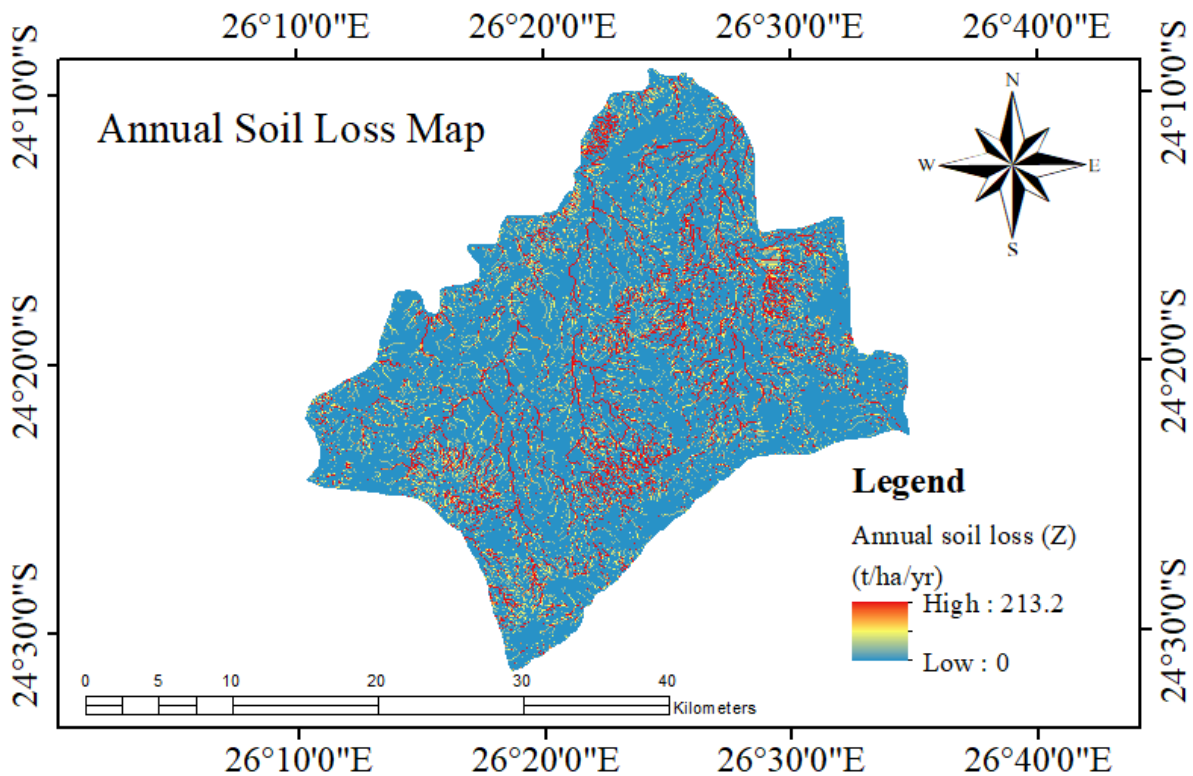


**Fig.4. 7 Spatial distribution of annual soil loss of Dinogeng**

#### 4.3.7 Potential Erosion Risk Analysis

The study area was classified into five soil erosion risk categories shown in Figure 4.8 following the work of Maronedze and Schütt (2020). The area and proportion of soil erosion risk classes are illustrated in Table 4.8. The estimated soil erosion risk averaged  $0.9 \text{ t ha}^{-1} \text{ yr}^{-1}$ . The maximum and minimum losses are ranging from about  $0 \text{ t ha}^{-1} \cdot \text{yr}^{-1}$  to  $213.2 \text{ t ha}^{-1} \cdot \text{yr}^{-1}$ . Eighty-eight percent of DAEA (69, 999 ha) has erosion risk of  $0 \text{ t ha}^{-1} \cdot \text{yr}^{-1}$  to  $2 \text{ t ha}^{-1} \cdot \text{yr}^{-1}$  (low to moderate). Only 2% (1905 ha) and 10% (7946 ha) of the study area experience very high to extreme soil erosion loss rate of  $5\text{-}10 \text{ t ha}^{-1} \cdot \text{yr}^{-1}$  and  $\geq 10 \text{ t ha}^{-1} \cdot \text{yr}^{-1}$  respectively. The spatial patterns of the estimated soil erosion risk indicate very high to extreme erosion risk areas are occurring along the streams, at steep slopes and areas of bare land such as the dry pan.

The topographic factor and soil erodibility are key determinants of soil erosion risk in the study area according to SLEMSA model. However, areas with a high slope are small compared to plain and flat areas. A larger portion of the study area is located on flat areas which experience low erosion. Topography and soil erodibility factors are among the natural

factors determining soil sensitivity to erosion. Vegetation is a human controlled factor and therefore by implementing conservation measures and preserving existing vegetation, erosion risks can be reduced to a great extent.

**Table 4.8. Estimated soil erosion risk in Dinogeng for 2020 LULC**

Erosion risk classes	Soil loss ( $\text{tha}^{-1}\text{yr}^{-1}$ )	Area (ha)	Percentage
<b>Low</b>	0 - 1	62521.0	75%
<b>Moderate</b>	1 - 2	7477.9	9%
<b>High</b>	2 - 5	3266.7	4%
<b>Very high</b>	5 - 10	1905.4	2%
<b>Extremely high</b>	>10	7946.0	10%

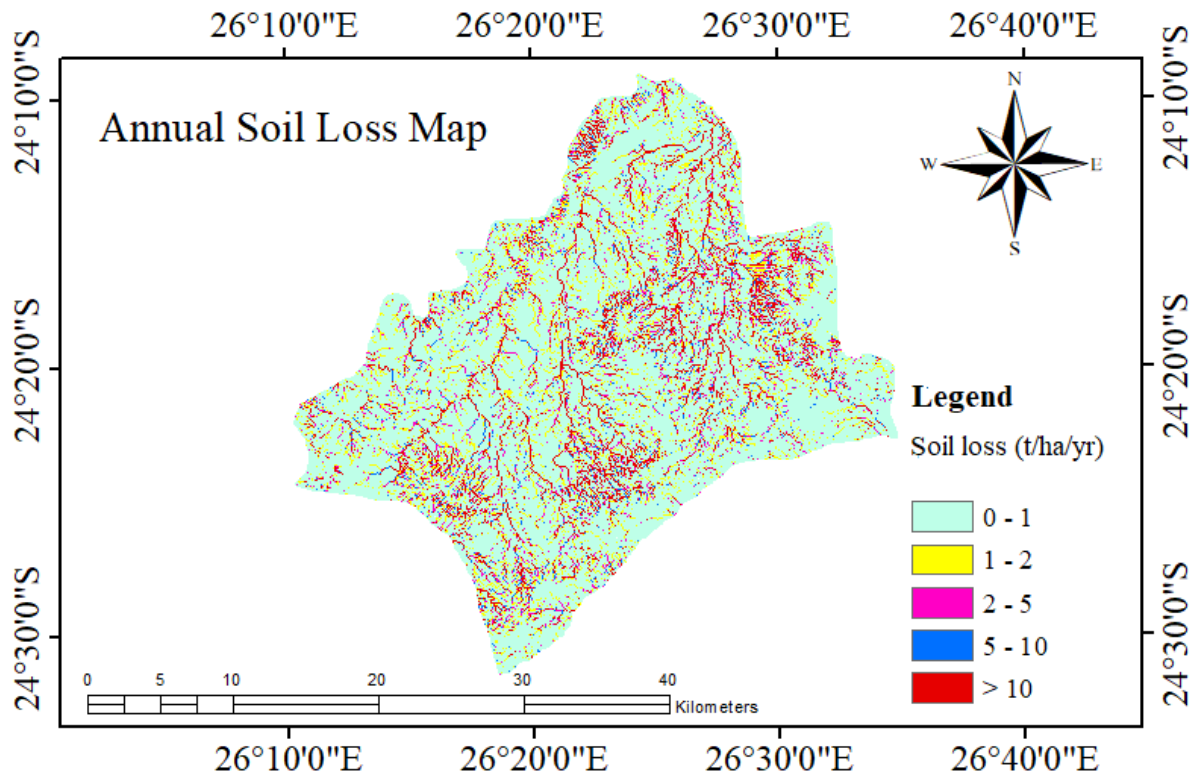


**Fig.4. 8 Soil erosion risk map for Dinogeng**

## CHAPTER 5: SUMMARY AND CONCLUSION.

Sustainable land management is essential for agricultural areas to get on upon land resource degradation problems. However, developing appropriate land management strategies is partly constrained by lack of reliable information and spatial distribution of the problem of land degradation at smaller scale like agricultural extension areas or farm level. The main objective of this study was to assess soil erosion risk and soil fertility changes in Dinogeng Agricultural Extension Area. This study was set out to specifically determine LULCC using GIS and RS for the period from 2006 to 2020; assess soil fertility changes for the period before and after inception of the ISPAAD programme and map out soil erosion risk areas for the 2020 LULC map using the geographic information system-interfaced with SLEMSA model. In general terms, ISPAAD has resulted into serious environmental impacts such as severe loss of natural vegetation, and decline in soil fertility and soil erosion.

In a 14-year span (2006 -2020), the LULC of Dinogeng changed markedly. LULC categories information before ISPAAD in 2006 was 19.7%, 11.5%, 7.2% and 61.6% for cultivated land, bare land, forested land and shrub land respectively. However, the land cover classes changed to 39.1%, 29.7%, 6.5% and 24.7% respectively in 2020 after ISPAAD for the same categories. The results show that expansion of cultivated land and bare land occurred at the expense of natural vegetation cover. Cultivated land and bare areas increased by 19.4 and 18.3 % whereas shrub land and forest areas decreased by 36.9 and 0.7 %, respectively. The results of this study are in agreement with other studies (Amsalu et al, 2006; Schneider and Pontius, 2001). Population increase and positive response by farmers towards the ISPAAD programme led to high demand for land for cultivation resulting in deforestation. Thus, sustainable and integrated land use management interventions are required to address the negative consequences of LULC dynamics in the study area.

The soil fertility assessment for the eighteen (18) selected farms in Dinogeng showed an average decline of 1.55 for pH, 0.16 % for OC and 6.75 Cmol/kg for CEC, as soil chemical properties. The overall results before and after ISPAAD generally show a decline in all the three soil parameters (Table 4.6). The pH of the baseline data ranged from 6.96 to 5.01 indicative of neutral to strongly acidic soils. After the inception of ISPAAD, pH ranged from 6.11 to 4.06 indicating slightly acidic to extremely acidic soils. The OC percentage ranged between 0.20 % (low) and 0.85% (sufficient) before ISPAAD, and between 0.02% (very low) and 0.75% (average enough) thereafter. Cation exchange capacity (CEC) values ranged between 2.00 – 15.00 Cmol/kg before, and between 0.80 – 5.62 Cmol/kg after ISPAAD.

Sandy soils generally have a very low CEC while heavier clay soils have a much higher CEC. The decline in soil fertility could be attributed to soil erosion and effects of continuous crop cultivation.

Acidification in the area of study could be attributed to availability of Soils with high sand content and/or low levels of soil organic matter and harvesting grains and crop residues from the land which removes considerable quantities of SOC content. Very few smallholder farmers' take advantage of applying fertilizers supplied under ISPAAD programme so there is less likelihood of acidification due to fertilizer application in the study area. The ISPAAD programme has led to intensification of crop cultivation on vulnerable soils resulting in nutrient losses. Soil fertility decline could be one of the most important constraints limiting food production and food security in Dinogeng.

In mapping soil erosion hazards, the integration of soil loss prediction model (SLEMSA) in geographic information system (GIS) was used to estimate the spatial distribution of soil loss in DAEA using the LULC map for 2020 satellite image. The results indicated that 88% of DAEA has low to moderate soil erosion risk ( $0 - 2 \text{ tha}^{-1}\text{yr}^{-1}$ ). Only 12% of the study area experience very high to extreme high erosion risk ( $5 - \geq 10 \text{ tha}^{-1}\text{yr}^{-1}$ ) along the streams, at steep slopes and areas of bare land. The results of the study have shown SLEMSA as a useful model to differentiate areas of high and low erosion potential.

This study has underscored the role of topography and soil erodibility, as natural factors, in driving soil erosion. As a larger portion of the study area is located on flat areas which experience low erosion, LULC (or vegetation) is a key human controlled factor affecting erosion and therefore implementing conservation measures and preserving existing vegetation can reduce erosion risks to a great extent. This study has also shown that GIS and RS technology is very useful and capable of detecting the changes in land use and land cover comprehensively. The study reveals that the LULC pattern and its spatial distribution are essential for the foundation of an appropriate land use management practices that promotes productive and sustainable use of soils and, in the process, minimizes soil erosion and other forms of land degradation.

## RECOMMENDATIONS

1. The findings gathered from this study can be used as the basis for development of a strategy, policy, programme, and extension services for implementing the following actions:
  - a) good agricultural and sustainable soil management practices
  - b) sustainable land use planning
  - c) soil conservation programme
2. Communities need to be educated on the importance of soil fertility management and soil erosion control practices for effective and efficient implementation of the programmes and policies.
3. Areas of very high and extremely high erosion risk require adequate erosion control practices to be implemented on a priority basis in order to conserve soil resources.
4. Where possible, communities should be encouraged to consider land use for biofuels and forest plantations to balance or reduce the negative effects of the expansion of cultivation and subsequent land degradation due to the ISPAAD programme.
5. This study identified the issue of soil acidification, which can potentially lower the availability of soil nutrients. It is recommended that the soils from these areas be routinely tested. Furthermore, an in-depth study on the influence of soil acidification on soil nutrient loss and its relation to different types of human activities is recommended.

## REFERENCES

- Abel, N. and Stocking, M. A. (1987). A rapid method of assessing rates of soil erosion from rangeland: An example from Botswana. *J. Range Management*, 40: 460-466.
- Agidew, A.A., & Singh, K.N. (2017). The implications of land use and land cover changes for rural household food insecurity in the Northeastern highlands of Ethiopia : the case of the Teleyayen sub - watershed. 6:56 DOI 10.1186/s40066-017-0134-4 *Agriculture & Food Security RESEARCH*. <https://doi.org/10.1186/s40066-017-0134-4>
- Alliance for Green Revolution in Africa(AGRA). (2014). *Africa Agriculture Status Report: Climate Change and Smallholder Agriculture in Sub-Saharan Africa*. Nairobi, Kenya.
- Amsalu, A, Leo, S, Jan de, G. (2006). Long-term dynamics in land resource use and the driving forces in Beressa watershed, highlands of Ethiopia. *Journal of Environmental management* 83: 13-32.
- Amuri, N., Semu, E., Msanya, B.M., Mhoro, L. Anthony, J. M. (2010). Evaluation of the soil fertility status in relation to crop nutritive quality in the selected physiographic units of Mbeya Region , Tanzania; Second RUFORUM Biennial Meeting 20 - 24 September 2010, Entebbe, Uganda Research Application Summary Evaluation p, (June 2014).
- Anand, A. (2018). Accuracy Assessment Unit 14: Processing and Classification of Remotely Sensed Images, (May).
- Annepu, S. K. Shirur, & Sharma, V. P. (2017). Assessment of Soil Fertility Status of Mid Himalayan Region , Himachal Pradesh. *Indian Journal of Ecology* (2017) 44(2): 226-231. Manuscript Number: 2503 NAAS Rating: 4.96., (August).
- Appiah, D.O., Forkuo, E.K., Bugri, J.T., & Apreku, T.O. (2017). Geospatial Analysis of Land Use and Land Cover Transitions from 1986 – 2014 in a Peri-Urban Ghana. *Geosciences* 2017, 7, 125; doi:10.3390/geosciences7040125. [www.mdpi.com/journal/geosciences](http://www.mdpi.com/journal/geosciences), 1–23. <https://doi.org/10.3390/geosciences7040125>
- BCA Consult (Pty) Ltd. (2012). *Poverty and Social Impact Analysis of the Intergrated Support Programme for Arable Agriculture Development ( ISPAAD )*. Final Report. GoB-UNDP-UNEP Poverty Environment Initiative (PEI). Gaborone, Botswana., (November).

- Bharatkar, P. S., & Patel, R. (2013). Approach to Accuracy Assessment for RS Image Classification Techniques: International Journal of Scientific & Engineering Research, Volume 4, Issue 12, December-2013 ISSN 2229-5518.
- Bobe, Bedadi. Woreka. (2004). Evaluation of Soil Erosion in the Harerge Region of Ethiopia Using Soil Loss Models, Rainfall Simulation and Field Trials by Bobe Bedadi Woreka Submitted in partial fulfilment of the requirements for the Degree Doctor of Philosophy : Soil Science in the, (July).
- Breetzke, G.D., Koomen E., and Critchley, W. R. S. (2013). GIS-Assisted Modelling of Soil Erosion in a South African Catchment: Evaluating the USLE and SLEMSA Approach: IntechOpen. Book Citation Index in Web of Science ,[http //dx.doi.org/10.5772/52314](http://dx.doi.org/10.5772/52314).
- Breitbart R. (1988). Soil Testing Procedures for Soil Survey Part 1 Theoretical background and modifications of standard procedures: Soil Mapping and Advisory Services Botswana. FAO, UN and GoB. AG : BOT/85/011 FIELD DOCUMENT 3.
- Bvindi, A. (2019). Assessment of soil erosion hazard around the abandoned Nyala mine in formerly Mutale Municipality, Limpopo Province, South Africa. A research thesis submitted to the Department of Geography and Geo-Information Sciences, School of Environmental Sciences at.
- Campbell J.B. and Wynne R.H. (2011). Introduction to Remote Sensing Fifth Edition. The Guilford Press, New York, London. [www.GISman.ir](http://www.GISman.ir) (Fifth Edit). London: Guilford Press.
- Chanda, R., Chipanshi, A.C., Totolo, O., & Magole, L. (1999). The Vulnerability and Adaptation to Climate Change of the Crops Subsector in Botswana: The Cases of Sorghum and Maize in the Barolong and Ngamiland Agricultural Districts, Draft Report: Department of Mines, Ministry of Water and Mineral Resources.
- Chen, F. W., & Liu, C. W. (2014). Estimation of the Spatial Rainfall Distribution using Inverse Distance Weighting (IDW) in the middle of Taiwan; ISSN 1611-2490 Volume 10 Number 3 Paddy Water Environ (2012) 10:209-222 DOI 10.1007/s10333-012-0319-1, (September 2012). <https://doi.org/10.1007/s10333-012-0319-1>
- Chen, F., & Liu, C. (2014). Estimation of the Spatial Rainfall Distribution Using Inverse Distance Weighting (IDW) in the middle of Taiwan. *Article*, (March).

<https://doi.org/10.1007/s10333-012-0319-1>

- Cheruto, M. C., Kauti, M.K., Kisangau, P. D., & Kariuki, P. (2016). Assessment of Land Use and Land Cover Change Using GIS and Remote Sensing Techniques : A Case Study of Makueni County , Kenya. *Journal of Remote Sensing & GIS*, 5:4 DOI: 10.4175/2469-4134.100017., 5(4). <https://doi.org/10.4175/2469-4134.1000175>
- Congalton, R. (1991). A review of assessing the accuracy of classifications of remotely sensed data. *Remote Sens Environ*; 37 : 35–46.
- Culman, S., Mann, M., & Brown, C. (n.d.). Calculating Cation Exchange Capacity , Base Saturation , and Calcium Saturation Fact Sheet.
- Deb, S.K. & Nathr, R. K. . (2012). Land use/cover classification- An introduction review and comparison; *Global Journal of researches in engineering Civil And Structural engineering* Volume 12 Issue 1 Version 1.0 January 2012 Type: Double Blind Peer Reviewed International Research Journal P, 12(1).
- Dube, F. (2011). Spatial Soil Erosion Hazard Assessment and Modelling in Mbire District, Zimbabwe : Implications for Catchment Management by Faculty Of Engineering, (July).
- Eastman, J. R. (2006). Guide to GIS and Image Processing. IDRISI Source Code ©1987-2006. IDRISI Production ©1987-2006 Clark University Manual Version 15.00, (April), 0–327.
- Elwell, H. A. (1978). Modelling soil losses in Southern Africa, *Journal of Agricultural Engineering Research*, Volume 23, Issue 2, 1978, Pages 117-127, ISSN 0021-8634, [https://doi.org/10.1016/0021-8634\(78\)90043-4](https://doi.org/10.1016/0021-8634(78)90043-4)., 23(2), 117–127.
- FAO, and. GoB. (2016). Food and Agriculture Organisation of the United Nations and Government of Botswana : Country Programming Framework for Botswana, 2014 - 2016.
- FAO, IFAD, W. (2013). The State of Food Insecurity in the World 2013. The multiple dimensions of food security. Rome, FAO.
- FAO. (2015). Status of the World’s Soil Resources (SWSR) – Main Report. Food and Agriculture Organization of the United Nations and Intergovernmental Technical Panel on Soils, Rome, Italy.

- FAO/IIASA/ISRIC/ISS-CAS/JRC. (2009). Harmonized World Soil Database; Version 1.1, FAO, Rome, Italy and IIASA, Laxenburg, Austria. March 2009.
- FAO. (1984). Fertilizer and Plant Nutrition Guide: FAO Fertilizer and Plant Nutrition Bulletin 9.
- FAO. (2008). Guide to laboratory establishment for plant nutrient analysis, FAO Fertilizer And Plant Nutrition Bulletin 19. ISBN 978-92-5-105981-4.
- FAO. (2010). Cultivating Sustainable Livelihoods : Socioeconomic Impacts of Conservation Agriculture in Southern Africa, REOSA Technical Brief, 1–6.
- Gete, Z, Hurni, H. (2001). Implications of land use and land cover dynamics for mountain resource degradation in the Northwestern Ethiopian Highlands. *Mountain Research and Development* 21: 184-191.
- Gray, J.M., Bishop, F.A.T., Wilson, B.R. (2016). Factors Controlling Soil Organic Carbon Stocks with Depth in Eastern Australia. *Soil Science Society of America Journal*, 79: 1741–1751.
- Grohs, F., and Elwell, H. A. (1993). Estimating sheet wash erosion from cropland in communal area of Zimbabwe. *Transactions of the Zimbabwe Scientific association*, 67: 6-12.
- Guo, J.H.; Liu, X.J.; Zhang, Y.; Shen, J.L.; Han, X.W.; Zhang, W.F.; Christie, P.; Goulding, K.W.T.; Vitousek, P. M. , & Zhang, F. S. (2010). Significant acidification in major Chinese croplands. *Science* 327, 1008–1010.
- Hano, A. I.A. (2013). Assessment of Impacts of Changes in Land Use Patterns on Land Degradation / Desertification in the Semi- arid Zone of White Nile State , Sudan , by Means of Remote Sensing and GIS, Thesis submitted to fulfill the partial requirements for degree of Doctor .
- Heydarnejad, S., Fordoei, A. R., Mousavi, S. H., & Mirzaei, R. (2020). Estimation of soil erosion using SLEMSA model and OWA approach in Lorestan Province ( Iran ); S. Heydarnejad et al. / *Environmental Resources Research* 8, 1 (2020) 9 *Environmental Resources Research* Vol. 8, No. 1, 2020, 8(1).
- Hoyle, F. (2013). *Managing Soil Organic Matter: A Practical Guide*, Grains Research and

- Development Corporation (GRDC), ISBN 978-1-921779-56-5 Published July 2013.  
Retrieved from [https://grdc.com.au/\\_\\_data/assets/pdf\\_file/0029/107696/grdc-guide-managingsoilorganicmatter-pdf.pdf](https://grdc.com.au/__data/assets/pdf_file/0029/107696/grdc-guide-managingsoilorganicmatter-pdf.pdf)
- Hurni, H. (2016). Erosion Productivity Conservation Systems in Ethiopia IV International Conference on Soil Conservation, Maracay, Venezuela, pp. 654 - 674 (1215 pp.), (January 1985).
- Igwe, C. A. Akamigbo, F. O. R.; Mbagwu, J. S. C. (1999). Application of SLEMSA and USLE Erosion Models for Potential Erosion Hazard Mapping in South-eastern Nigeria. *International Agrophysics*, 13(1):41-48.
- Jones, Clain Olson-Rutz, K. (2020). *Soil Acidification: Problems, Causes, & Testing*, Montana State University Extension.
- Joshua, W. D. (1991). *Physical Properties of the Soils of Botswana : Soil Mapping and Advisory Service Botswana*. FAO-GoB-UNDP; AG : BOT/85/011 Field Document 33.
- Kavitha & Sujatha. (2015). Evaluation of soil fertility status in various agro ecosystems of Thrissur District , Kerala , India, 328–338.
- Kayombo, B.,Moulenmberg, F.,Moganane, B.G., Dikinya, O., Aliwa, J.N., Nsinamwa, M., Gaboutloeloe, G., Patric, C., Mzuku, M., Machacha, S. (2005). Characterisation of Agriculture Land Degradation in Botswana; *Botswana journal of technology* pg 1 - 8.
- Ketterings, Q. Reid, S and Rao, R. (2007). *Cation Exchange Capacity (CEC); Agronomy Fact Sheet Series; Fact Sheet 22*, Department of Crop and Soil Sciences, Cornell University.
- Ketterings, Q.M., Albrecht, G., & Beckman, J. (2005). *Soil pH for Field Crops; Agronomy Fact Sheet Series; Fact Sheet 5*; College of Agriculture and Life Sciences, Department of Crop and Soil Sciences.
- Kgatlang District Council. (2002). *Kgatlang District Development Plan 6 : 2003 - 2009, Aligned to NDP9: Theme 'Towards Realisation of Vision 2016' Sustainable and Diversified Development Through Competitiveness in Global Markets.*, pp 201.
- Lal, R. (2018). Digging deeper: A holistic perspective of factors affecting soil organic carbon sequestration in agroecosystems. *Global Change Biology (Early View)*, <https://doi.org/10.1111/gcb.14054>.

- Lambin, EF, Geist, H. (2001). Global land-use and land-cover change: what have we learned so far. *Global Change Newsletter* 46: 27-30.
- Lillesand, T.M., Kiefer, R.W., & Chipman, J.W. (2015). *Remote Sensing and Image Interpretation Seventh Edition*: John Wiley & Sons, Inc., 111 River Street, Hoboken, NJ 07030-5774, (201) 748- 6011, fax (201) 748-6008, website [www.wiley.com/go/](http://www.wiley.com/go/).
- Liu, X., Shi, H., Bai, Z., Liu, X., & Yang, B. (2018). Assessing Soil Acidification of Croplands in the Poyang Lake Basin of China from 2012 to 2018, 1–12.
- Maida, J.H.A., Chilima, Z.W. (1976). Changes in Soil Fertility under continuous cropping of Tea: Technical Bulletin No. 1/Bv/76. Bvumbwe Research Station, Limbe, Malawi.
- Manandhar, R., Odeh, I. O.A., & Ancev, T. (2009). Improving the Accuracy of Land Use and Land Cover Classification of Landsat Data Using Post-Classification Enhancement; *Remote Sens.* 2009, 1, 330-344; doi:10.3390/rs1030330 ; [www.mdpi.com/journal](http://www.mdpi.com/journal). <https://doi.org/10.3390/rs1030330>
- Maronedze, A. K., & Schütt, B. (2020). Assessment of Soil Erosion Using the RUSLE Model for the Epworth District of the Harare Metropolitan Province, Zimbabwe; *Sustainability* 2020, 12, 8531; doi:10.3390/su12208531.
- McCauley, A., Jones, C., & Jacobsen, J. (2005). *Basic Soil Properties: Soil and Water Management Module 1*, Montana State University, 1–12.
- Merritt, W.S., Letcher, R.A., Jakeman, A. J. (2003). A review of erosion and sediment transport models. *Environmental Modelling and Software*, 18:761- 799.
- Ministry of Agriculture. (2013). *Guidelines for Intergrated Support Programme of Arable Agriculture Development (ISPAAD)*. Revised version May 2013., (May), 1–24.
- Mishra, S., Shrivastava, P., & Dhurvey, P. (2017). Change Detection Techniques in Remote Sensing: A Review. *International Journal of Wireless and Mobile Communication for Industrial Systems*, 4(1), 1–8. <https://doi.org/10.21742/ijwmcis.2017.4.1.01>
- Mkonda. (2017). Yields of the Major Food Crops : Implications to Food Security and Policy in Tanzania ’ s Semi-Arid Agro-Ecological Zone. <https://doi.org/10.3390/su9081490>
- Moesi, M. S. (2021). Integrating GIS and remote sensing in estimation of soil loss using the

SLEMSA and RUSLE models: A case study of Taung Watershed, Ramotswa Agricultural District: A dissertation submitted to the Department of Agricultural & Biosystems Engineering, (July).

Morgan, R.P.C., & Davidson, D. (1991). Soil erosion and conservation. Longman Group, UK.

Morgan, R. P. C. (2005). Soil Erosion and Conservation Third Edition; BLACKWELL PUBLISHING 350 Main Street, Malden, MA 02148-5020, USA 108 Cowley Road, Oxford OX4 1JF, UK 550 Swanston Street, Carlton, Victoria 3053, Australia.

Mugabe, W., Akanyang L., Nsinamwa M., Moatswi B., Matthews N., Dipheko, Ujjan I.A., and . S. A. A. (2017). Fodder Tree Species Composition and Density in Grazing Gradients of Fenced and Unfenced Grazing Areas of the Gaborone North, Botswana;, (June). <https://doi.org/10.17582/journal.sja/2017/33.2.306.314>

Ohio State University Extension (OSU). (2004). Ohio Agronomy Guide 14th Edition Bulletin 472.

Omuto, C. T. Vargas, R. (2018). Soil Nutrient loss Assessment in Malawi Technical Report; Food and Agriculture Organization of the United Nations and the UNDP-UNEP Poverty-Environment Initiative and the Ministry of Agriculture, Irrigation and Water; ISBN 978-92-5-131142-4 (FAO) Developm.

Parece, T., Campbell J., & McGee, J. (2011). Remote Sensing in an ArcMap Environment, Manual, pp 263.

Paris, S. (1990). Erosion hazard model (modified SLEMSA). Field document no 13, second version, land resource evaluation project, Malawi, 17 pp.

PCI Geomatics Enterprises. (2018). Geomatica II Training Guide Version 2018.

Rammelzwaal, A. (1989). Soil and Land Suitability for Arable Farming of South-East Central District : Soil Mapping and Advisory Service Botswana. AG: BOT/ 85/011. Field Document 7. GoB-FAO-UNDP.

Rammelzwaal, A., & Verbeek, K. (1990). Revised General Soil Legend of Botswana. FAO/UNDP/Government of Botswana. Soil Mapping and Advisory Services Project. AG: BOT/85/011. Field Document 32, 75pp., pp 81.

- Renard, K.G. Laflen, J.M., Foster, G.R., McCool, D. . (1994). The Revised Universal Soil Loss equation. In: Lal R. (ed.), *Soil Erosion Research Methods* (2nd edition), pp. 105-124.
- Ross, S. M. (1993). Organic matter in tropical soils: current conditions, concerns and prospects for conservation. *Progress in Physical Geography: Earth and Environment*, 17(3):265-305.
- Rumpel, C. & Kögel-Knabner, I. (2011). Deep soil organic matter – a key but poorly understood component of terrestrial C cycle. *Plant and Soil*, 338: 143-158.
- Rwanga, S., & Ndambuki, J M. (2017). Accuracy Assessment of Land Use / Land Cover Classification Using Remote Sensing and GIS. *International Journal of Geosciences*, 8, 611-622. <https://doi.org/10.4236/ijg.2017.84033>, 2017, 611–622.  
<https://doi.org/10.4236/ijg.2017.84033>
- SADC. (2016). *Outcome of the SADC Ministerial Workshop : Towards a Poverty Free and Food Secure Future*. Gaborone, Botswana., (May), 1–6.
- Schneider, LC, Pontius, R. (2001). Modeling land-use change in the Ipswich watershed, Massachusetts, USA. *Agriculture, Ecosystems and Environment* 85: 83-94.
- Schulze, R. E. (1979). Soil Loss in the Key Area of the Drakensberg – A Regional Application of the ‘Soil Loss Estimation Model for Southern Africa’ (SLEMSA). In: *Hydrology and water resources of the Drakensberg*. 149-167.
- Seanama Conservation Consultancy. (2012). *Agriculture and Food Security Policy Brief Reflecting on the Challenges of Attaining a Green Economy for Botswana*. GoB-UNDP. pp 1 - 7, 1–7.
- Seleka. (1999). The performance of Botswana’s traditional arable agriculture : growth rates and the impact of the accelerated rainfed arable programme ( ARAP ), 20, 121–133.
- Shahzeidi, S. S., Entezari, M., Gholami, M., & Dadashzadah, Z. (2019). Assessment Rate of Soil Erosion by GIS ( Case Study Varmishgan , Iran ) *J. Basic. Appl. Sci. Res.*, 2(12)13115-13121, 2012, (January 2012).
- Smith, H. . J. (1999). Application of Empirical Soil Loss Models in southern Africa: a review, *South African Journal of Plant and Soil*, DOI: S. Afr. J. Plant Soil 1999,

16(3),158-163., 1862. <https://doi.org/10.1080/02571862.1999.10635003>

Statistics Botswana. (2016). Botswana Environment Statistics 2016; Statistics Botswana Publishers, Gaborone. Website: <http://www.statsbots.org.bw>, pp 90.

Statistics Botswana. (2014). Population and Housing Census 2011 Analytical Report. Government Printer, Gaborone (pp 1 - 506). Email: [csobots@gov.bw](mailto:csobots@gov.bw) Website: [www.cso.gov.bw/cso](http://www.cso.gov.bw/cso).

Statistics Botswana. (2015). Annual Agricultural Survey Report 2013. Email: [info@statsbots.org.bw](mailto:info@statsbots.org.bw) Website: [www.cso.gov.bw](http://www.cso.gov.bw).

Stocking, M., Chakela, Q., & Elwell, H. (1988). An Improved Methodology for Erosion Hazard Mapping Part I : The Technique; *Geografiska Annaler. Series A, Physical Geography*, Vol. 70, No. 3 (1988), pp. 169- 180. *Published by: Wiley*, (June 2018), pp 164. <https://doi.org/10.2307/521069>

Tersteeg J.L. (1993). Land Resources and Production Systems in Agricultural Land Use Planning in Botswana: Land Use Planning for Sustainable Agricultural Development, BOT/91/001, Technical Paper 4, FAO - Government of Botswana - United Nations Development Programme., (June).

Tesfamichael S.G. (2004). Mapping Potential Soil Erosion Using RUSLE , Remote Sensing , and GIS : The Case Study of Weenen Game Reserve, KwaZulu-Natal; Thesis: Submitted in partial fulfilment of the requirements for the Degree of Master of Science in Applied Environmental Sciences., (May), pp 146.

Tiruneh, G., and Ayalew, M. (2015). Soil Loss Estimation Using Geographic Information System in Enfranz Watershed For Soil Conservation Planning IN Highlands Of Ethiopia; *Int. J. Agril. Res. Innov. & Tech.* 5 (2): 21-30, December, 2015 ISSN: 2224-0616; Available at <http://www.ijarit.webs.com>, 5(2), 21–30.

Tshireletso, K., Makhabu, S. W., Nsinamwa, M. Kgosiesele, E. Setlalekgomo, M. R., & Seletlo, Z. Majaga, S. & Legwatagwata, B. (2018). Diversity Patterns of Woody Vegetation of Kgatleng District , Botswana, In: *Climate change and adaptive land management in southern Africa – assessments, changes, challenges, and solutions* (ed. by Revermann, R., Krewenka, K.M., Schmiedel, U., Olwoch, J.M., (January).

- United States Department of Agriculture (USDA) Natural Resources Conservation Service. (1998). Soil Quality Indicators pH :Soil Quality Information Sheet Soil; USDA, (January).
- Vargas, R. & Omuto, C. (2016). Soil loss Assessment in Malawi ; Food and Agriculture Organization of the United Nations and the UNDP-UNEP Poverty-Environment Initiative and the Ministry of Agriculture, Irrigation and Water Development, Malawi. Food and Agriculture Organization of the United Nations and the UNDP-UNEP Poverty-Environment Initiative and the Ministry of Agriculture, Irrigation and Water Development, Malawi.
- Wingqvist G.O. and Dahlberg E. (2008). Botswana Environmental and Climate Change Analysis: Environmental Economics, University of Gothenburg, Brief desk study Sida INEC, Stockholm, (April), pp 1-21.
- Wischmeier W.H. and Smith D.D. (1978). Predicting Raifall Erosion Losses; A guide to Conservation Planning: United States Department of Agriculture Handbook, (Handbook No. 537), pp 67.
- World Bank Group. (2015). Botswana Poverty Assessment: World Bank Group Poverty Report No. 88473-BW, Poverty Global Practice Africa Region, (March).

## APPENDICES

### Appendix 1: Interpretation of Kappa statistics

S. No	Kappa statistics	Strength of agreement
1	< 0.00	Poor
2	0.00 - 0.20	Slight
3	0.20 - 0.40	Fair
4	0.40 - 0.60	Moderate
5	0.60 - 0.80	Substantial
6	0.80 - 1.00	Almost perfect

---

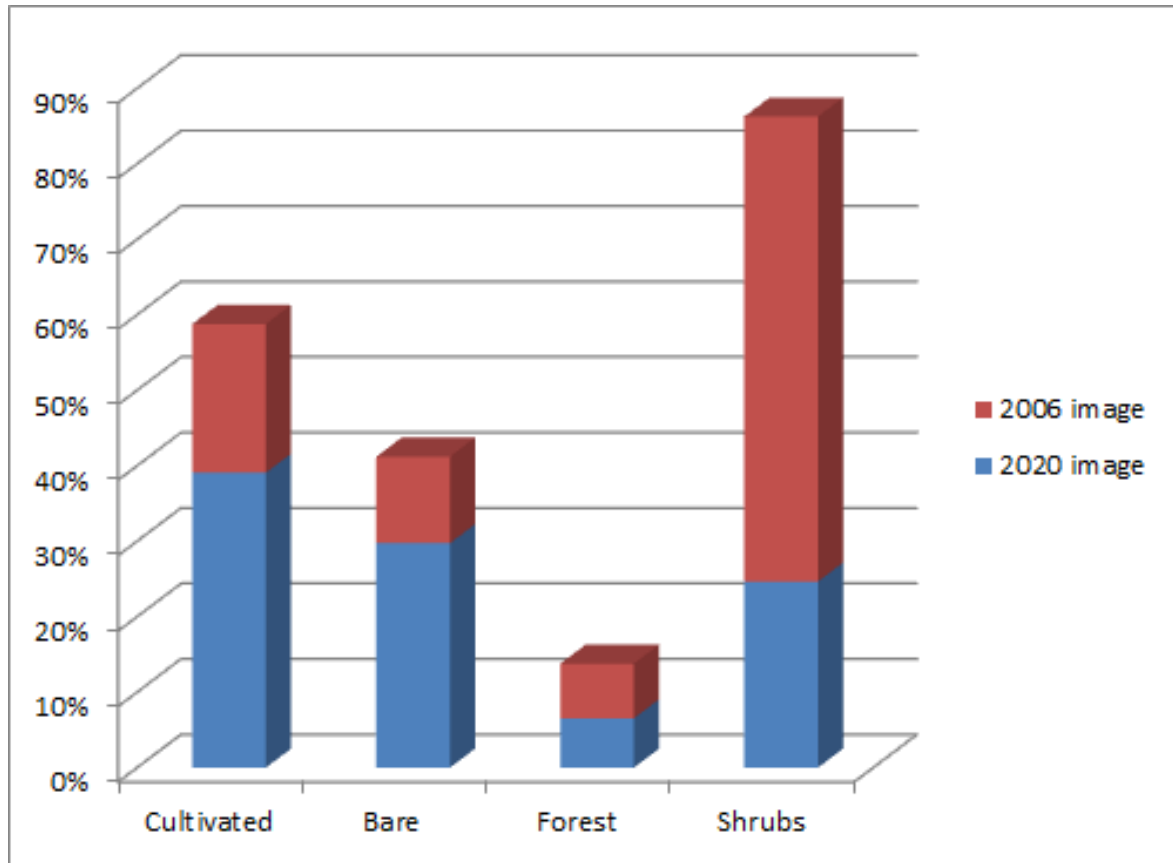
**Source:** (Rwanga and Ndambuki, 2017)

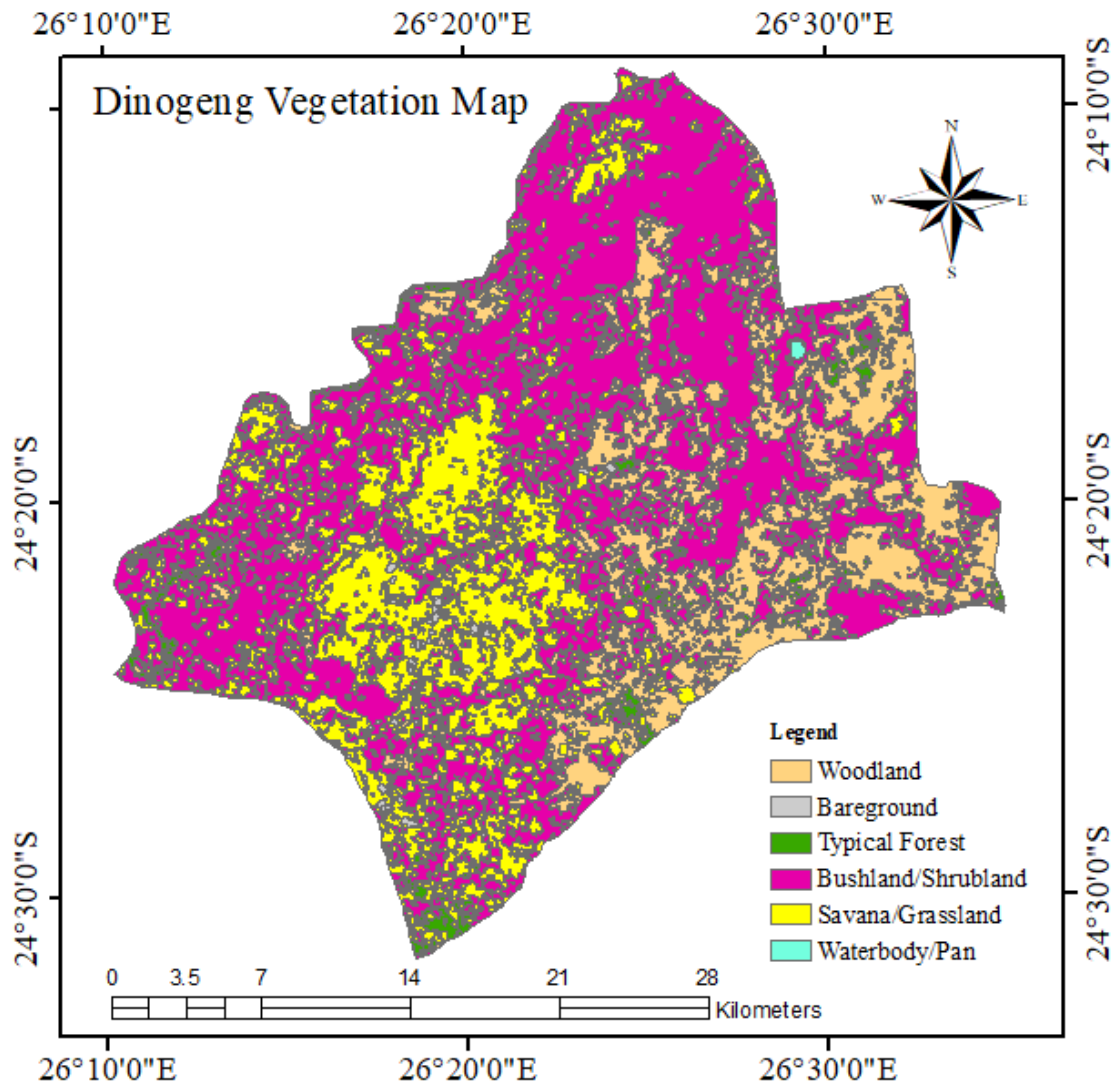
### Appendix 2: Error Matrix Summary Table (2006 and 2020)

	Expected				Overall accuracy	Kappa coefficient	
	C	NC	Total	UA			
Observed	C	224	14	238	0.94		
	NC	16	226	242	0.93		
	Total	240	240	480			
	PA	0.93	0.94				
	Overall accuracy					0.94	
	Kappa coefficient						0.88

**C:** Correct, **NC:** Not correct, **UA:** User's accuracy, **PA:** Producer's accuracy

**Appendix 3: Bar chart depicting LULCC in percentage.**



**Appendix 4: Vegetation map of the study area**



**Appendix 6; Various change detection techniques**

<b>CHANGE DETECTION TECHNIQUE</b>	<b>BEST SUITED FOR</b>
Post classification	Land use land cover classification and change, Urban Sprawl measuring, Change detection by unsupervised classification.
Image rationing	Monitoring changes in environment using LANDSAT.
Image differencing	Urban land cover changes at the urban fringe from SPOT HRV imagery, Change detection in forest ecosystems.
Principal component analysis	Brush-fire damage and vegetation regrowth, Land- cover change, land-use change detection and analysis.
Direct multi date classification	Land-cover change detection
Change vector analysis	Land cover monitoring, Land-Use/ Land-Cover Change Detection, Forest change detection, Disaster assessment

Source: (Mishra et al., 2017)

**Appendix 7: Average annual rainfall in mm (2000-2019) Mochudi station**

Year	July	August	September	October	November	December	January	February	March	April	May	June	Annual total
2000/01	0	0	0	24	19.1	49	110	224	74.5	20	5.3	12	537.5
2001/02	0	0	0	157	240	16	10	245	56.3	30.7	79	10	843.4
2002/03	0	0	0	0	9.5	102	14	43	34.5	18.5	20	0	241.2
2003/04	0	0	0		54.3	36	0	33	0	0	0	10	133.3
2004/05	0	0	0	10	159	92	61	65.2	49.3	29.8	0	0	465.4
2005/06	0	0	0	0	7	93	14	24	21	15	0	0	173.4
2006/07	0	0	0	0	27.5	48	162	214	123	0	0	0	573.8
2007/08	0	0	0	43.5	32.5	79	67	0	15	14.8	0	23	274.3
2008/09	0	0	0	0	81	0	145	2	149	10	10	0	396.9
2009/10	0	0	8	20.7	117	28	228	72	105	0	53.2	77.5	709.7
2010/11	0	0	0	0	54.7	145	0	35.2	79.5	213	3.2	0	530.6
2011/12	0	0	0	2.2	28.2	86	177	0	96	42	0	0	431.8
2012/13	0	0	0	41.5	44.5	21	99	31.6	51	0	0	0	287.7
2013/14	0	0	0	7	82	103	37	73.3	168	9	0	0	478.9
2014/15	0	0	0	7	92.5	70	71	22	33	3	0	0	298.5
2015/16	0	0	0	5.5	32	33	30	18	58.8	16	0	15	208.1
2016/17	0	0	0	30.5	146	9	201	319	5.5	34	0	0	744.4
2017/18	0	0	0	0	0	49	20	107	14.5	52.8	0	0	243.5
2018/19	0	0	0	0	3	32	37	8	0	40	0	0	120.3
												Average	404.9

Source: Department of Meteorological Services, Ministry of Environment, Natural Resources Conservation and Tourism

**Appendix 8: Average annual rainfall in mm (1995-2019) Olifantsdrift station**

Year	July	August	September	October	November	December	January	February	March	April	May	June	Annual total
1995/96	0	0	0	17	50.1	47	86	37	109	14	38	0	397.1
1996/97	0	0	63.9	29	47.9	128	54	0	82.5	0	0	0	405.5
1997/98	0	0	0	35	47.5	144	15	45	24	0	33	0	344
1998/99	0	0	0	7.5	23.2	137	192	100	95	14	6	24	598.9
1999/00	0	0	0	36.5	68	80	18	122	22.1	10.5	37	7	400.5
2000/01	0	0	0	77	223	13	23	139	30.3	14.5	34	0	553.8
2001/02	0	0	0	0	54	63	27	32	22	0	0	13	211
2002/03	0	0	0	108	41	17	127	139	130	58	0	0	620.2
2003/04	0	0	0	9	23.4	136	81	15	23	32.3	0	0	319.9
2004/05	0	0	0	0	22	56	128	114	36	32.3	8	0	396.1
2005/06	0	0	0	0	30.6	129	46	0	54	29	0	14	302.8
2006/07	0	0	0	49.5	112	93	123	99	137	23	0	0	635.9
2007/08	0	0	0	0	89.2	46	119	81	44	0	0	0	378.6
2008/09	0	0	0	55	99.8	0	195	40	0	238	0	0	627.4
2009/10	0	0	0	0	50	39	134	0	92.8	0	0	0	315.7
2010/11	0	0	0	16.5	27	162	0	n/a	108	0	0	0	314.1
2011/12	0	0	0	5.5	0	3	3	0	n/a	75	0	0	86.5
2012/13	0	0	0	0	18.6	106.6	118	60	53.7	0	0	0	250.3
2013/14	0	0	0	0	0	134.6	26	0	6.5	0	0	0	32.7
2014/15	0	0	0	0	23	26	38	59	74	0	0	0	220
2015/16	0	0	0	14	23.7	10	57	37	0	0	0	0	141.3
2016/17	0	0	0	0	n/a	n/a	n/a	n/a	n/a	0	0	0	0
2017/18	0	0	0		n/a	n/a	55	58	0.5	0	0	0	112.7
2018/19	1.4	0	0	0	14	58	17	7.6	0	60	0	0	158
												Average	326

Source: Department of Meteorological Services, Ministry of Environment, Natural Resources Conservation and Tourism

**Appendix 9: Average annual rainfall in mm (1995-2019) Sikwane station**

Year	July	August	September	October	November	December	January	February	March	April	May	June	Annual total
1995/96	0	0	0	21	190	98	144	155	19	18	28	0	673.5
1996/97	0	0	0	12	62.3	54	122	26	233	38	31.5	0	578.8
1997/98	0	6.2	46	9.7	63	47	69	52	83	0	0	0	375.2
1998/99	0	0	0	24	79	260	67	16	13	32	31	0	521
1999/00	0	0	0	7.3	6	75	53	144	57.5	8	4	38	393.1
2000/01	0	0	0	53	39	60	123	240	55	49	79	7	704.6
2001/02	0	0	0	66.5	158	44	34	10	0	17	39	0	367.8
2002/03	0	0	0	0	0	10	50	92	6	0	0	0	158
2003/04	0	0	0	70	50	55	66	91.5	70	14	0	0	416
2004/05	0	0	0	18	50	136	61	25	54	0	0	0	343.5
2005/06	0	0	0	0	48	47	217	230	26.7	16	0	0	584.7
2006/07	0	0	0	0	16.2	75	20	0	5.5	26	0	24.5	166.7
2007/08	0	0	0	62.9	46.5	92	238	17	125	0	0	0	580.4
2008/09	0	0	0	0	89.2	0	83	52	96.2	0	0	0	320.4
2009/10	0	0	0	35.8	104	59	154	19.3	30.8	120	26.2	0	549.7
2010/11	0	0	0	25.5	25.5	105	136	7.5	105	34.4	10	0	448.5
2011/12	0	0	0	25	3	92	88	0	56.9	n/a	n/a	n/a	264.8
2012/13	0	0	0	24.6	62.5	0	16	0	13	4.4	0	0	120.5
2013/14	0	0	0	33	11	145	0	48	53.6	10.5	0	0	301.1
2014/15	0	0	0	37	38.8	149	22	0	0	6.7	0	0	253.3
2015/16	0	0	0	3.5	30	13	41	46	135	0	0	0	268.4
2016/17	0	0	0	68.1	74.2	15	91	41	0	0	0	0	289.3
2017/18	0	0	0	0	0	2.5	23	62.4	19	0	0	0	107.2
2018/19	0	0	0	0	0	45	40	24.2	0	60	0	0	168.8
												Average	373.1

Source: Department of Meteorological Services, Ministry of Environment, Natural Resources Conservation and Tourism